공학석사학위논문

The effects of composition and thickness on the optical properties and hardness of Al-Si-N films deposited by RF magnetron sputtering

RF magnetron sputtering 으로 증착한 Al-Si-N 박막의 조성과 두께가 광학성질과 경도에 미치는 영향

2019 년 08 월

서울대학교 대학원
재료공학부
리타 마리아

The effects of composition and thickness on the optical properties and hardness of Al-Si-N films deposited by RF magnetron sputtering

RF magnetron sputtering 으로 증착한 Al-Si-N 박막의 조성과 두께가 광학성질과 경도에 미치는 영향

지도교수 박 찬

이 논문을 공학석사학위논문으로 재출함
2019 년 08 월

서울대학교 대학원
재료공학부
리타 마리아

리타 마리아의 석사학위논문을 인준함
2019 년 08 월

위 원 장: 유 상 임 (인)
부위원장: 박 찬 (인)
위 원: 김 진 영 (인)

Abstract

The effects of composition and thickness on the optical properties and hardness of Al-Si-N films deposited by RF magnetron sputtering

Rita Maria Carmen Galvez

Department of Materials Science and Engineering

The Graduate School

Seoul National University

Electronic devices with displays such as cellular phones, smart watches and navigational devices are some of the most widely used everyday items. These devices experience much wear and tear due to daily use. Since the display is an important part of these devices, it is necessary to find ways to improve its overall performance to increase its lifetime. One such way is to apply hard coatings on the surface of the displays.

Hard coatings, which are coatings that have high hardness and good wear resistance, have been used to protect different items such as tooling devices and mechanical parts like engines. Although widely used in various industries, only a few materials have been applied to optical devices such as displays since most of the hard coating materials are not transparent in the visible range. Most optical hard coatings applied in glass currently are those

with hardness up to ~12 GPa. It is important to find other possible materials that can provide higher hardness and high optical transparency at low thicknesses. Al-Si-N has been a material of interest due to its good properties. Al-Si-N has been found to have high values of hardness while maintaining a high degree of transparency in the visible range. The nanocomposite structure of the film provides enhance hardness values.

In this study, the effect of composition and thickness of Al-Si-N films deposited by RF reactive magnetron sputtering on Gorilla Glass (which is currently used in smart phones) on the optical transparency and hardness were studied. The effect of films with four different compositions were determined, and it was found that as the silicon content was increased, the hardness of the films was decreased. This can be due to the differences of the microstructures of the films with different silicon contents. The highest hardness obtained from the films with lowest silicon content can be attributed to the nanocomposite structure of the film.

Films with ~0.6 μm, ~0.8 μm, and ~1 μm thicknesses were also deposited to determine the effects of thickness. All films were found to have similar silicon contents of ~15 at %, which is within the typical range of silicon content for nanocomposite structures. SEM results show the grainy morphology of the surfaces with grain sizes smaller than 100 nm while XRD results show the presence of AlN crystalline phase in the film. These results show the nanocomposite structure of the film, and the enhanced hardness can be attributed to this structure.

All films were also found to have similar hardness and optical transmittance levels. Even at a thickness of ~0.6 μm, the films retain their high hardness values around 22 GPa and have a measured transmittance up to ~90%, which is similar to that of Gorilla Glass substrate. This shows that Al-Si-N films as thin as ~0.6 μm can be used as a hard coating with hardness up to 22 GPa on Gorilla Glass which is widely used as the cover glass of the smart phones used today.

Keywords: Al-Si-N, hard coatings, Gorilla Glass, hardness, optical properties, transparency, sputtering

Student Number: 2017-21243

Contents

1. Introduction

Electronic devices which has displays such as cellular phones, smart watches and navigational devices are some of the most important and used items in the world. These devices undergo much wear and tear due to its everyday use. The displays or screens of the devices is one of the most used, if not the most used, part of these devices.

According to a survey conducted by the Allstate subsidiary SquareTrade in 2018, roughly 5,761 phone screens are broken every hour in the US alone. Two out of three Americans reported damaging their phones within one year before the survey wherein 29% reported cracked screens and 27% reported scratched screens. These broken phone screens cost these consumers more than $3.4 billion in repairs and replacements per year in the US. [1, 2] It is necessary to find ways in order to reduce the occurrence of broken devices due to its importance in everyday life.

As the displays of the devices are some of the most used yet at the same time, most damaged part, it is necessary to improve the mechanical properties or protect the display to increase the lifetime of the devices and to improve its overall performance.

Also, the screen to body ratio of these devices, particularly cell phones, have steadily been increasing. Other parts such as finger print sensors and speakers have been incorporated with the displays in order to

accommodate larger displays. [3] With this, protecting the screens also means protecting other important parts of the devices.

One method that is currently being studied is the use of hard coatings or films to protect the displays of the devices. These coatings are used to prevent cracks and scratches from forming on the displays. Hard coatings are coatings with high hardness that are widely used in different industries to improve product performance, lifetime, and overall manufacturing and reduce maintenance costs. [4] They are applied to tooling devices such as drill bits to improve wear resistance, automotive engines to increase gas mileage by reducing wear and consequently friction that can be detrimental to gas consumption. [5]

Since these coatings would be used for the displays, these coatings should have high hardness and be highly transparent at the same time. Most available hard coatings used in the market today are not transparent in the visible range. Most of the commonly used hard coatings such as transition metals like nitrides or carbides are mostly opaque in nature when they are thicker than ~50 nm. This is due to their unsaturated valence band electrons. [6] Thus other materials that have the required transparency should be investigated.

Silicon dioxide, silicon nitride, and aluminum oxides are some of the materials currently used as hard coatings for optical devices. These are also being used for display applications. [7-15] Since the hardness values of these materials are only up to 12 GPa, and these films may also need to be

processed at temperatures that can be detrimental to the cover glass of the display, there is a need to determine whether other materials that can be deposited at lower temperatures can provide a high hardness value while still maintaining high transparency. The possibility of depositing films maintaining high hardness and high transparency at low thicknesses (≤ 1 μm) should also be investigated.

Al-Si-N have been of great interest for optical applications because it is known to have high hardness and high optical transparency. It has been reported that films of 1-10 μm thicknesses have hardness values up to 30 GPa while having transparencies above 70%. [6, 16-26] Although Al-Si-N has been studied and deposited on quartz for applications such as spacecraft windows, studies on electronic device displays, particularly on Gorilla Glass has not yet been explored.

In this study, the feasibility of applying Al-Si-N hard coatings of thickness of ~0.6 μm to ~1 μm through RF reactive sputtering and the effects of composition and thickness on the hardness and transparency are explored. The power and substrate temperature used during sputtering and the silicon content of the films were optimized to grow films with high transmittance and high hardness. Results show that it is possible to deposit Al-Si-N films as thin as ~0.6 μm that have transparencies of up to ~90% and hardness of up to 22 GPa. Films with thicknesses ranging from ~0.6 μm to ~1 μm have similar hardness and transmittance levels. The resulting hardness and transparency

at this small thickness shows that, with further research, Al-Si-N can be applied as a hard coating for electronic device displays.

2. Background

2.1 Hard coatings

Hard coatings are widely used to protect tools and equipment such as tooling bits in different industries. These tools are used under harsh working environments which can include different chemicals, very high temperatures, high contact pressures and high cutting speeds. Hard coatings are applied to protect tools from wear and tear and increase its lifetime and performance. [5]

The term “hard coatings” can be used generally to comprise all coatings that provides a required protection or resistance to a certain environment or factors such as optically hard, radiation hard, and electrically hard coatings. But traditionally, the term is used to refer to coatings with high hardness in the mechanical sense. [27]

Hard coatings can be deposited through chemical vapour deposition (CVD) or physical vapor deposition (PVD) techniques which includes magnetron sputtering and arc evaporation. [5, 28]

2.1.1 Hard coatings on electronic devices

Transparent hard coatings are currently being used on displays of some electronic devices. These hard coatings are used to protect the cover glass, which is usually the other most layer of the displays. The application of the hard coatings improves upon the hardness of the cover glass. For which has values of around 6-7 GPa. [29]

These coatings should not only have higher hardness than that of glass, but also maintain the transparency of the display. Current hard coatings used includes aluminium oxide, silicon dioxide, silicon nitrides, and other polymeric materials such as acrylates.

Aluminum oxide is currently being used by Apple on their iPhone and Mac devices. [13] It involves laser annealing deposited amorphous Al_2O_3 to create a hard film. The current reported hardness of Al_2O_3 films is up to 12 GPa and they are deposited with thicknesses up to 2 μm. Transmittance levels for these films have been reported to be around 80%. [11, 14]

Silicon dioxide coatings are also being used on cover glass. When applied during manufacturing, they are usually used for anti-reflection purposes but studies have also shown that it also improves the hardness of glass of values up to 9 GPa. Usual thicknesses applied on glass are around 2 μm and transmittance levels can be higher than 90%. [7, 9, 10, 12]

Polymeric materials are also used as hard coatings, particularly when devices use polymeric substrates on their displays. These polymeric materials include acrylates which are cured on top of the substrates to form coatings to protect the displays. These coatings have reported hardness of ~4H using pencil tests. These films are of 5-250 μm thicknesses and have reported transmittance levels of around 80% in the visible range.[8, 15]

Even with hardness values of up to 12 GPa, there are still many reported cases of scratched and cracked screens. [1, 2] It is necessary to find other materials that can possess higher hardness but maintain or even improve upon current transparency levels of the applied hard coatings.

In addition, applying these films would possibly need temperatures of up to 1000^{o}C during application or post-treatments which could damage the cover glass. Gorilla Glass has a strain point of 571^{o}C, the temperature in which the properties of the glass start to change. [29] Thus it is not just necessary to find a new material that could have high hardness and transparency levels but it is also important that this material is possible to be deposited in lower temperatures.

It would also be beneficial if thinner films or coatings are used to reduce production time and to limit the amount of materials needed to be consumed.

2.2 Nanocomposite Hard coatings

Nanocomposite films have many possible applications such as oxidation resistant, antibacterial, hard coatings, temperature stable, etc. They have gathered great interest due to the possibilities of enhanced physical and chemical properties such as high hardness, high optical transparency, and high corrosion resistance. [19, 22]

These nanocomposite films usually are made out of at least two phases, at least one nanocrystalline phase and an amorphous phase. The phases should also be refractory for the produced nanostructure to be stable. [19]

Particularly, nanocomposite films have been studied due to the possibility of high hardness. [5, 28] These films have shown great wear resistance in laboratories. [28] In these hard nanocomposite films, the nanocrystalline phase is surrounded by another phase, which results in films with higher hardness. [20] The basic morphology of the film can be seen in Fig. 1.

In order to create nanocomposite films with high hardness, it should be a two-phase material with sufficiently small nanocrystallites which are embedded in a thin matrix phase. The nanocrystallites should be sufficiently small to prevent dislocation movement. It should also be present in a thin matrix to prevent crack propagation. The interfaces between the phases

should also be strong and sharp so that grain boundary sliding is prevented. [30]

The properties of these nanocomposite films are dependent on their structure, phase composition, and also their nano-morphology. The nanomorphology of the film, which includes the size of the grains, not only allows for enhanced properties but can also result in new unique properties for the film.

Nanocomposite films have been reported to be deposited through both CVD and PVD methods. [28, 30]

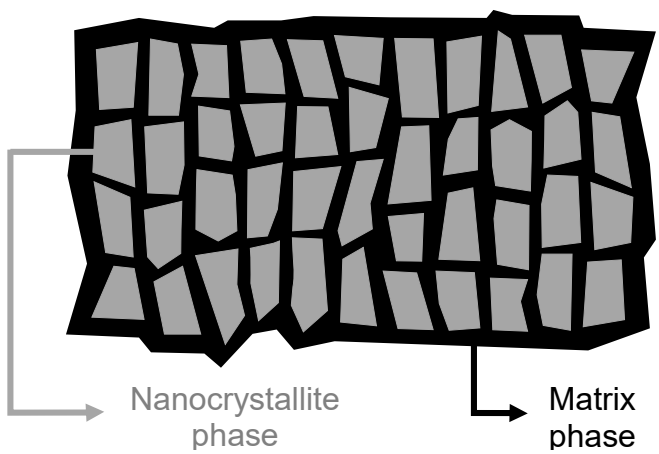

Figure 1. Nanocomposite film morphology

Ti-Al-N, Ti-Al-C-N, Zr-Ti-N, and other transition metal nitrides or carbides hard nanocomposite films have already been studied. [20] These films are used for coatings on tooling items improve both product performance and lifetime. Although possessing high hardness, these films would not be applicable for optical applications due to their opaqueness since they are metallic in nature and their unsaturated valence band electrons make them opaque for thicknesses higher than 50 nm. [6]

In order to create films with the required transparency, the combination of group III nitrides such as AlN, BN, and GaN as the nanocrystalline phase and SiNx as the amorphous phase was studied. Among the possible combinations, Al-Si-N has been found to not only possess high hardness, but also has high transparency which is required for optical applications.

2.3 Al-Si-N

Al-Si-N is a nanocomposite system that was found to have high hardness while being transparent in nature. This system is a combination of aluminum nitride (AlN) and silicon nitride (SiN_x/ Si_3N_4) phases which both have hexagonal crystal structures.

Aluminium and silicon nitrides, unlike other metal nitrides used for hard coatings, are found to be transparent in the visible range. AlN has been

chosen among the group III nitrides since it possesses the widest bandgap of 6.2 eV. [24] Si_3N_4 also has a band gap of 5.5 eV, which is similar to that of AlN. [31] Having a wide band gap is advantageous for transparency as more light, especially of lower wavelengths which have higher energies, are able to pass though the material and not be absorbed. [32] Due to this property, they possess the required optical transparency which is needed for optical applications.

AlN is also found to have good optical properties and possess good mechanical and anti-oxidation properties. It can also be easily deposited through PVD processes, particularly sputtering. [24]

Al-Si-N has already been investigated for potential applications as optical coatings with tailored refractive indices, anti-oxidation coatings, UV light emitters, and field emission devices. [24, 33] It was also investigated for is high thermal stability. [21] It has been reported to be deposited on quartz, glass, silicon, and stainless steel. [6, 16-26]

2.3.1 Effect of Silicon Content

The amount of silicon incorporated in the films has been reported to affect the structure of the film and the resulting mechanical properties. The properties, especially the hardness of the film, can depend on the structure of the film. Depending on the morphology, the hardness of the film can be

due to different hardening mechanisms [19, 24]. Studies show that increasing the silicon content of the Al-Si-N films up to a certain value leads to an increase of hardness.

According to the reports of Pelisson et al., increasing the silicon content of the films up to around 10 at % can increase the hardness up to 30 GPa. [24] Any further increase to the silicon content decreases the hardness of the films. The changes in the hardness of the films is highly dependent on the structure of the film, which changes with varied silicon content.

Pelisson et al. described the structure of the Al-Si-N films with increasing silicon content. The group explained that Al-Si-N films at lower silicon content are of $Al_{1-x}Si_xN$ solid solutions. After a certain solid solution limit, in their study 6 at %, Si atoms starts to segregate out of the AlN lattice and form a separate Si_3N_4 amorphous phase [6]. This was also reported by Kasu et al. with the deposition of Al-Si-N using chemical vapor deposition at high temperatures. [34] They have reached this conclusion since results show the decrease of the AlN lattice parameter with increasing Si content up to 6 at %. The decrease in the lattice parameter is due to the substitution of the silicon atoms in the AlN lattice. The decrease in the AlN lattice parameter stopped at 6 at %. [24]

It was shown that at low silicon content, the enhanced hardness of the films was explained through the Hall-Petch effect of the nanocrystallites. As the silicon content increases up to 6 at %, the nanocrystallites become

smaller and the hardness is due to a competition between grain boundary sliding and solid solution hardening.

At silicon content above 6 at %, a second amorphous Si_3N_4 phase is formed and the enhanced hardness is due to the nanocomposite structure of the film. As the grain size continues to decrease with increasing silicon content, the hardness is expected to stop increasing and decrease further due to the increasing effect of grain boundary sliding with grain refinement. [24]

In another report by the same group, they further clarified the structures formed as the silicon content is further increased. As the silicon content is increased from 7 to 12 at %, the crystallite size decreases while having the same amount of amorphous phase surrounding the crystallites. As the concentration is further increased from 12 at %, the nanocrystallites do not change size and the amorphous phase starts to increase its coverage. From this silicon content, the films should not be considered to be an Al-Si-N nanocomposite but a solid solution of Al in amorphous $S_{i3}N_4$. [6] This was also observed by Musil et al. in their samples of films with high silicon content. [22] The evolution of the structure of the films is visualized in Fig. 2.[6]

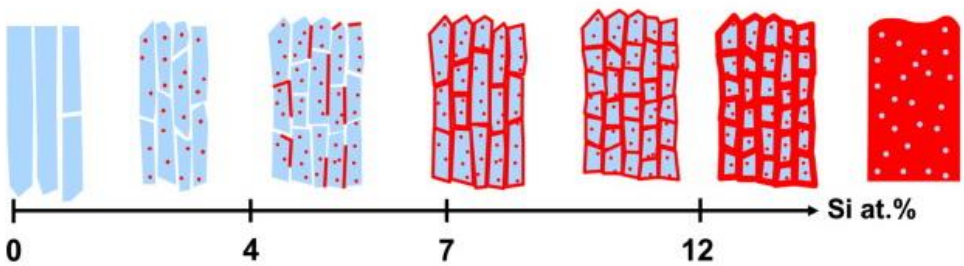

Figure 2. Illustration of the different microstructures of the Al-Si-N films at different Si concentrations. [6]

In silicon contents covering the $A_{lx-1}Si_xN$ solid solution, the hardness enhancement is due to the Hall-Petch effect. At silicon contents range of the nanocomposite structure, the hardness enhancement is due to the nanostructure hardening phenomenon. As the silicon content is further increased, grain boundary sliding increases due to grain refinement and the hardness is expected to decrease. [24]

The limit between the different morphologies has not been fully agreed upon. Reports by Liu et al. reported that it is possible for silicon to substitute for aluminium in the AlN lattice up to 8 at% when sputtered and silicon can replace aluminium in epitaxially grown $Al_{1-x}Si_xN$ up to 12 at%. The group also reported that films with silicon content of up to 35 at% may still be of nanocomposite structures.

Previous studies have reported on the effect of silicon content on the properties of the Al-Si-N film. Pelisson et al., have reported that in silicon contents from 0 to 25 at %, there is a faint hardness maximum of 30 GPa at 10 at % Si. [24] In a study by Musil et al. wherein they compared films with low (≤10 at %) silicon content with films with high (≥ 20 at %) silicon content, they showed that the films with high silicon content have higher hardness. Films with low silicon content were reported to have hardness values of up to 13.3 GPa while films with high silicon content of similar thickness were reported to have hardness values of up to 24.3 GPa. [22] The difference was also reported to be due to the change from solid solution in low silicon content to nanocomposite structure in higher silicon contents. Even with higher

silicon content, they have reported that their films were still of the nanocomposite structure. Liu et al. reported that a maximum hardness of 27 GPa was seen at silicon contents of around 25 at %. Their films were also reported to be of nanocomposite structure. [19]

The differences in the microstructure and hardness with silicon content between the different studies can be attributed to the different deposition methods and parameters used. Liu et al. used a typical laboratory magnetron sputtering setup while the other studies used higher energy magnetron processes. [19]

Aside from the influence on hardness, the influence of silicon content on the transparency of the films has also been reported by Pelisson et al. [24] The group reported that there is no influence of the silicon concentration of the film on the transparency of the film of silicon content of 2.5 to 18 at %.

2.3.2 Effect of Thickness

The thickness of any film can affect its properties. These properties can include the film's hardness and transparency.

It has been reported that with some films, there is a direct relation between thickness and grain size. [35] This change can lead to differences in the properties of the film.

With increasing thickness, it is known that the optical band gap of thin films decreases. The optical band gap shows the required excitation of electrons from the valence band to the conduction band through photons. As the band gap decreases, the transparency levels can also decrease. [36] Also, when transparent thin films are deposited onto a substrate, interference is bound to happen due to the interaction of the reflected light from the air-film and film-substrate interfaces. In the report by Pelisson et al., oscillations were present in films of different silicon content. These oscillations were explained by the presence of the films. [6]

The properties of the interference pattern produced by the films is a function of the wavelength of the light being reflected and by the properties of the film, particularly its thickness. [37-39] These properties include the amplitude and the spacing of the interference fringes.

The differences in the amplitude, or the maximum and minimum transmittance of the films is highly dependent on the film thickness. [38] As the thickness of the films increases, the amplitude of the film decreases. The fringe spacing also decreases with increasing thickness. [40]

Previous reports have shown this rule. Bozhko et al. reported that glass with Al-Si-N films of 0.9 to 6.2 μm thicknesses have retained their transparency and have similar transmittance levels. Although similar, as the thickness increased, the amplitude of the films decreased and the fringe spacing also decreased. The group also showed that there is a slight decrease in the maximum transmittance as the thickness increased. The

absorption edge also moved to longer wavelengths as the thickness increased. The group reported transmittance values of up to ~80%. [17] Another report by Bozhko et al. also reported the same trend in film thicknesses of 4.3 to 20.5 μm. They reported that this can be associated with the growth of AlN nanocrystal grain size with the increase of thickness. [16] A report by Mishra et al. also presented the same trend in thicknesses of 0.167 to 1 μm. [20]

The effect of thickness of Al-Si-N films on hardness has also been reported. Bozhko et al. reported the hardness values of films of thickness 0.9 to 6.2 μm thicknesses and showed no trend with the hardness. The deposited films were of similar hardness levels ranging from 24.8 to 26.6 GPa. [17]

Most studies on Al-Si-N focuses on thicknesses above 1 micrometer. It is important to investigate the possibility of applications of Al-Si-N films at lower thicknesses. The deposition of thinner films means less materials will be use and the films can be deposited at a faster speed. This means that manufacturing costs can be significantly decreased.

2.4. Deposition of Al-Si-N

Al-Si-N has been reported to be deposited using different methods such as reactive DC magnetron sputtering, chemical vapor deposition, reactive cathodic arc evaporation, and RF magnetron sputtering. [33]

Out of all the methods, magnetron sputtering is an efficient method of depositing nanocomposite films. Ease of control of deposition parameters as well as the ease in scaling up for industrial applications are reasons why it is the preferred method. [41]

2.4.1. RF Reactive Magnetron Sputtering

Al-Si-N films can be easily deposited through RF reactive magnetron sputtering.

Sputtering is a process where a target or source material is bombarded and sputtered by energetic ions, usually of inert gas such argon, generated in a glow discharge plasma. [42] After being ejected from the target, sputtered materials are then deposited onto a substrate. Typically, the film that is deposited on the film has the same or similar stoichiometry and composition to that of the target. [43] Typically, the kinetic energy of the bombarding ions in sputtering is higher than that of typical evaporated particles, which is a factor in obtaining films with uniform thickness and even coverage. [44] Secondary electrons are also produced from the target surface due to the ion bombardment. These electrons are important in maintaining the plasma in the system.

Reactive sputtering involves sputtering films in mixtures of both argon and a reactive gas, typically oxygen or nitrogen. This allows the combination

of not just the elements of the target, but also the element of the reactive gas. This allows for the deposition of compound films like oxides and nitrides.

Magnetron sputtering uses magnets behind the negative cathode to create a strong magnetic field that traps bombarding ions near the target which allows for faster sputtering of atoms from the target. [45, 46] This process also allows for a more stable high-density plasma that improves the efficiency of the sputtering process. [43] Magnetron sputtering also is easy to control and suitable for large-scale film deposition. [45] It is considered as one of the most effective process for the deposition of a wide range of thin film systems and is now the method of choice for many industries. [42, 43, 47]

RF magnetron sputtering is preferred over DC magnetron sputtering since the former can induce higher energies in the deposition system which can improve on the properties of the deposited film. RF sputtering involves alternating the electric potential of the current in the system at radio frequencies, usually at 13.56 MHz, to avoid charge build-up on the surface of the target. Over time, produced positive ions are accumulated on the surface which are removed using the alternating current.

The combination of the magnetron and RF systems produces higher sputtering yields and deposition speeds which are important for high product throughput. [48] RF magnetron sputtering is advantageous in the deposition of non-conductive materials. A basic schematic diagram of the RF magnetron system can be seen in Fig. 3. [43]

When depositing Al-Si-N films, great precaution should be done as it has been shown that the properties of the films are dependent on the deposition parameters. [26, 49] Deposition parameters include the power delivered by the RF or DC power source, pressures of sputtering and reactive gases, substrate temperature, etc.

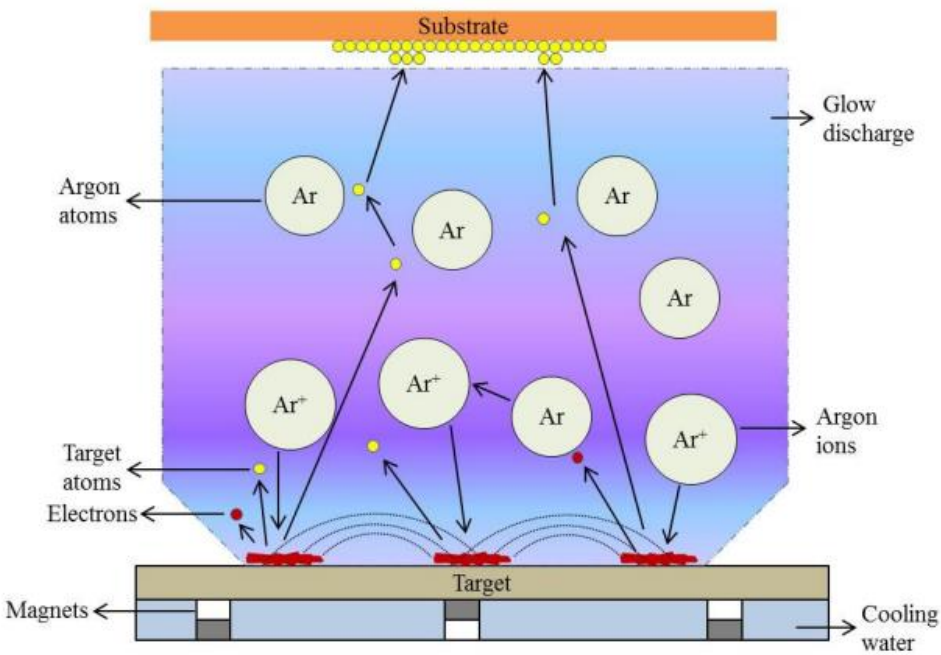

Figure 3. Basic Schematic Diagram of the RF magnetron sputtering process [43]

2.4.1.1. Effects of Power

The power given to the target during deposition is an important parameter. It plays an important role in deposition rate, crystalline quality, and other properties of the sputtered film. [50] Thus, the power used during deposition should be optimized to obtain films of desirable properties.

In RF sputtering, the use of higher RF powers makes the argon ions from the plasma to have higher kinetic energy or be more energetic. This also makes the sputtered atoms to have higher energy as well. [51] Since the bombarding ions have more energy, more material will be sputtered out from the target which will result in higher sputtering yield and thus, deposition rates.

Increasing the power is also known to produce smoother films. Differences in power can also lead to different crystallinity and preferred crystalline orientations of the deposited films. [52]

In the reports by Musil et al. It has been shown that films that were deposited with higher energy have higher transmittance in the visible range. They have reported that films sputtered at high energy has a dense, void-free microstructure. [22]

In the report by Pelisson et al., it was found that the power density has no influence on the grain size of the film. [24] Musil et al. also reported

that films deposited at low and high energies have similar hardness levels. [22]

2.4.1.2. Effects of Substrate Temperature

Substrate temperature can be a factor in changes of the microstructure of the deposited film. Depending on the temperature, a more crystalline or amorphous film can be produced. The temperature needed to change the structure of the film depends on the material being deposited.

In the reports of Pelisson et al., Al-Si-N films deposited at 200^{o}C and 500^{o}C with different silicon content were compared. [6, 24] In one study, the deposited films had a silicon content from 0 to 23 at% and were of 1-2μm thickness. It was reported that even with the difference in substrate temperature during deposition, there were no obvious influences of the temperature to the structure and mechanical properties of the film. Even as the hardness values at different silicon content varies, the hardness of the films deposited at the same silicon content but different substrate temperatures were similar.

In another study by the same group, they found no influence of the substrate temperature with the nanocrystallite size. This could explain why the substrate temperature has no significant influence on the hardness of the

films. The difference in the temperatures used in the studies may not be enough to produce any significant differences to the film.

3. Experimental Procedures

The experimental procedures are of two parts. The first part is to optimize the sputtering parameters which includes deposition temperature, power, and silicon content. The second part is to determine the effects of the thickness on the hardness and optical properties of the film.

Al-Si-N films were prepared through RF reactive magnetron sputtering using an aluminium-silicon (AlSi) composite target. Nitrogen (N_2) is used as the reactive gas during the deposition. An image of the sputtering set-up is seen in fig.4.

A composite target is used due to the limitation of having only one RF power source in the available sputtering set-up. Although it is possible to use the available direct current (DC) power source, problems can occur. A combination of separate Al and Si targets have been tested, where one RF and one DC power source were used. A composite target was also tested using the available DC power source.

Figure 4. RF Reactive Magnetron Sputtering set-up

Arcing occurred to the target attached to the DC power source during sputtering. This is due to the formation of an electrically insulating compound layer on the surface of the target due to the reaction of the surface with the nitrogen gas. This causes charge build-up on the surface that leads to arcing. Arcing can damage the target and produce uneven sputtering of the targets which produces films of unwanted composition, structure, and properties. [42, 53] Arcing can also destroy and create a rough surface of the target. [54] Since a non-conductive compound is formed on the surface of the target, there is a need to use RF power source to prevent charge build-up, and arcing, on the surface.

In order to deposit Al-Si-N films, Al-Si composite targets were used. The Al-Si composite target was prepared by attaching Si pieces of 10 mm x 10 mm size to a 99.9999% purity 2-inch diameter Al target.

For all depositions, the rotation speed of the deposition stage was set at 10 rpm to ensure an even deposition on the substrates. The base pressure of the deposition chamber was set at ~10^{-6} Torr while the process pressure was 1.5 x 10^{-3} mTorr. The argon and nitrogen flows were 4 sccm and 2.4 sccm respectively for all depositions.

Before each deposition, the targets were pre-cleaned with Ar gas for 7 minutes to remove any impurities on the surface of the targets.

3.1. Optimization of Sputtering Parameters

3.1.1. Optimization of Power

The sputtering power to be used in further experiments was first determined. To choose the sputtering power to be used, the deposition rate of the Al-Si-N films formed at different power levels were determined and compared.

Al-Si-N films were deposited for 10, 20, and 30 minutes per power level. The thickness of each film was determined through ellipsometry (JA Woollam Co, Inc.) and the slope of the fitted trend line was determined to get the deposition rate using each power.

The Al-Si-N films were deposited using 300 and 450 W. 450 W was set as the high value as this is the maximum power output of the available RF power source. All films were deposited at room temperature and an Al-Si composite target with one attached Si wafer piece was used.

3.1.2. Optimization of Silicon Content and Substrate Temperature

To determine the substrate temperature and the silicon content to be used in the study, the transmittance and hardness values of the films were determined and compared.

After optimizing the power to be 450 W, films of different Si content were deposited by using composite targets with different number of Si pieces attached. Al targets with one, two, three, and four Si pieces were used to determine the optimized silicon content. The targets used may be seen in fig. 5.

Films of similar thicknesses must be deposited in order to compare the transmittance and hardness of the films. The deposition rate using each composite target was first determined to control the thickness of the deposited films. After the deposition rates were determined, films of ~0.77 μm thicknesses were deposited.

Figure 5. AlSi Composite targets with different number of Si wafer pieces

The transmittance levels of the films were determined through UV-Vis spectroscopy. The transmittance levels from 240 to 1100 nm of each films were measured. The substrate temperature and silicon content to be used in future experiments was determined through comparing the transmittances of the films.

The hardness values of the films were measured through nano-indentation (TI 750 Ubi Hysitron). The hardness values of the films were measured with nano-indentation load of 6000 μm which produced nano-indentation depths of 100-150 nm. The silicon content to be used was determined by comparing the hardness levels of the films.

3.2. Deposition of films with different thicknesses

Al-Si-N films of three different thicknesses were deposited in order to determine the effects of thickness on the hardness and transparency of the films.

Films of three different thicknesses of optimized silicon content were prepared. Films of ~0.6 μm, ~0.8 μm, and ~1 μm were deposited by changing the deposition time during sputtering.

The Al-Si-N films were deposited on Corning Gorilla Glass as well as on SUS 301 stainless steel to aid in analysis.

3.2.1 Scanning Electron Microscopy (SEM) analysis

To determine the thickness of the films, the cross-section of each film was analysed using a field emission scanning electron microscope (FESEM, JEOL-7600F) by analysing the fractured cross-section surface of the films. The surface morphologies of selected samples were also analysed.

Films that were deposited on stainless steel were analysed through an electron dispersive system (EDS) attached to an FESEM (MERLIN Compact) to attain the relative composition of Al, Si, and N of the films. The analysed films were deposited on stainless steel (SUS 301) to help improve the accuracy of the analysis as glass contains silicon that can hinder with the analysis.

3.2.2. X-ray Diffraction (XRD) analysis

The x-ray diffraction patterns of the films were determined through X-ray diffraction (Bruker D8 Advanced). The XRD scans were done in grazing incidence (GI) mode for thin films with 0.5 step per second, from 10 to 80 degrees, with increments of 0.04 degrees. Select film samples were also scanned from 30-75 degrees, with increments of 0.02 degrees.

3.2.3. UV Vis Spectroscopy Analysis

The transmittances of the films deposited on Gorilla Glass from 250 to 1100 nm were measured through UV-Vis spectroscopy (Perkin Elmer Lambda 25).

3.2.4. Nano-indentation Analysis

The hardness values of the films were determined using a nano-indenter machine (TI 750 Ubi Hysitron). A maximum load of 6000 μN was applied to all films and indentation depths of 100 to 175 nm were produced.

4. Discussion

4.1. Optimization of Deposition Parameters

4.1.1. Effects of Power

To determine the power level to use during depositions, films were deposited using 300 W and 450 W and the deposition rate were compared. The thickness of the films deposited at 10, 20, and 30 minutes are seen in table 1. The thickness versus time graph was plotted and the slope of the fitted trend line was determined to get the deposition rate using each power. The plotted graphs and the fitted trend lines are seen in fig. 6. The deposition rates we determined to be 13.1 nm/min and 19.2 nm/second for 350 W and 450 W respectively.

The deposition rate increased with the increase of power. As the power increases, the ions bombarding on the target have more energy which results in more material being sputtered out from the target. This resulted in a higher sputtering yield which in turn, produced higher deposition rates.

Table 1. Thickness versus time measurements for 300 W and 450 W

Time (mins)	Thickness (nm)	
	300 W	**450 W**
10	138	192
20	276	331
30	384	610

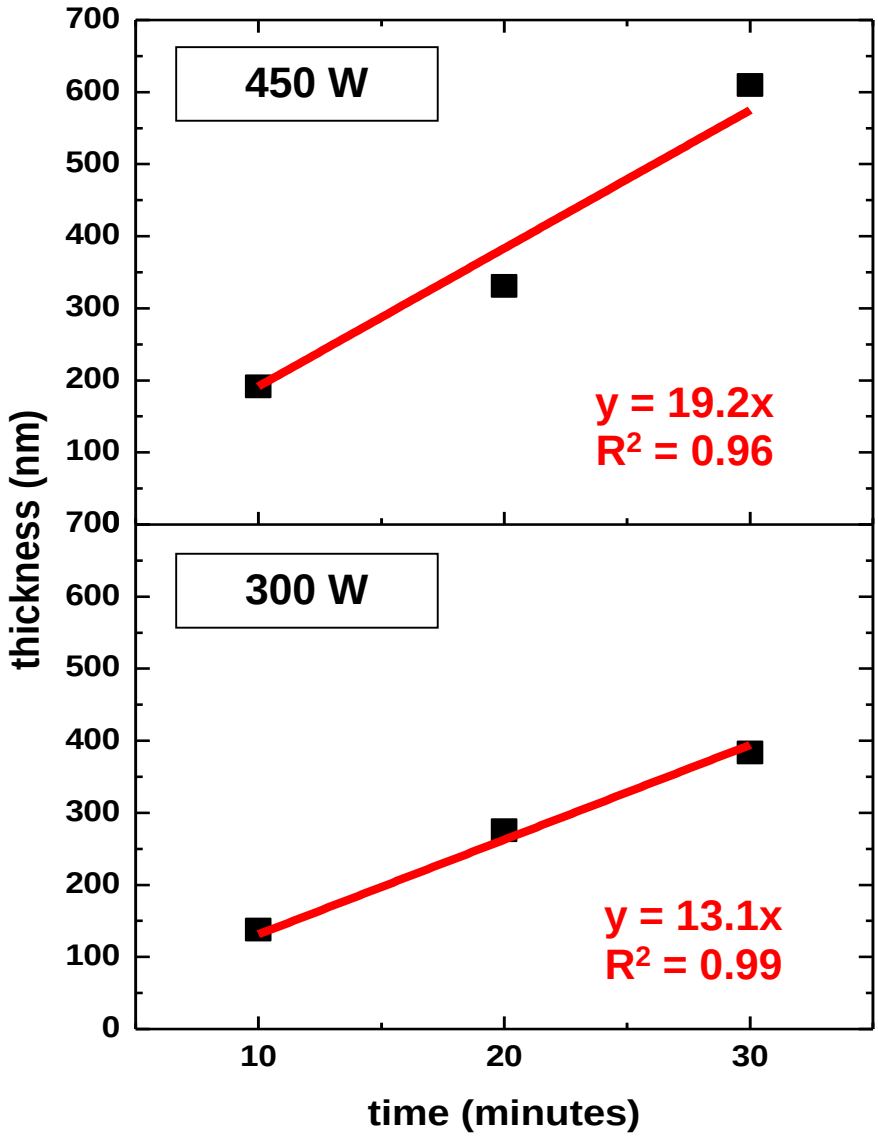

Figure 6. Thickness versus time of Al-Si-N films deposited using AlSi-1 target using different powers

4.1.2. Effects of Silicon Content and Substrate temperature

Al-Si-N films of different silicon contents were deposited using different substrate temperatures to determine the effect of the silicon content and substrate temperature. AlSi composite targets with different number of attached Si pieces were used to deposit films of different silicon content. Composite targets with one, two, three, and four pieces of silicon pieces attached are labelled as AlSi-1, AlSi-2, AlSi-3, and AlSi-4, respectively. Consequently, samples deposited using AlSi-1, AlSi-2, AlSi-3, AlSi-4 are labelled as AlSiN-1, AlSiN-2, AlSiN-3, and AlSiN-4 respectively. Samples are also deposited with similar thicknesses to aid with analysis.

The deposition rate of the films deposited using each target was first attained. The deposition rate is needed in order to deposit films of similar thickness. The thickness of the films deposited at 5, 10, 15, and 20 minutes are seen in Table 2. The thickness versus time graphs per target was plotted and the slope of the fitted trend line was determined to get the deposition rate using each power. The plotted graphs and the fitted trend lines are seen in fig. 7. The deposition rates were determined to be 12.6 nm/min, 16.1 nm/min, 17.0 nm/min, and 17.7 nm/min for AlSi-1, AlSi-2, AlSi-3, and AlSi-4 respectively.

Table 2. Thickness of deposited film per time per target

	Film Thickness (nm)			
Time (mins)	**AlSiN-1**	**AlSiN-2**	**AlSiN-3**	**AlSiN-4**
5	88	91	95	101
10	147	180	182	195
15	197	254	258	282
20	230	300	330	331

As the amount of silicon increases, the deposition rate also increased. This can be due to the differences in formation energy between AlN and Si_3N_4. AlN has a formation energy of -1.595 eV while Si_3N_4 has a formation energy of -1.312 eV. [31, 55] Since Si_3N_4 has a lower formation energy, Si_3N_4 can be deposited faster. As the amount of silicon present in the system increases as the number of Si pieces attached to the Al target increases, not only should the Si content of the deposited film increase, but also the deposition rate.

After determining the deposition rates, films with different silicon content were deposited using substrate temperatures of room temperature and 200^{o}C. The thicknesses of each film deposited at RT can be seen in Table 3 and films while films deposited at 200^{o}C can be seen in Table 4. The thickness of each film is plotted in Fig. 8.

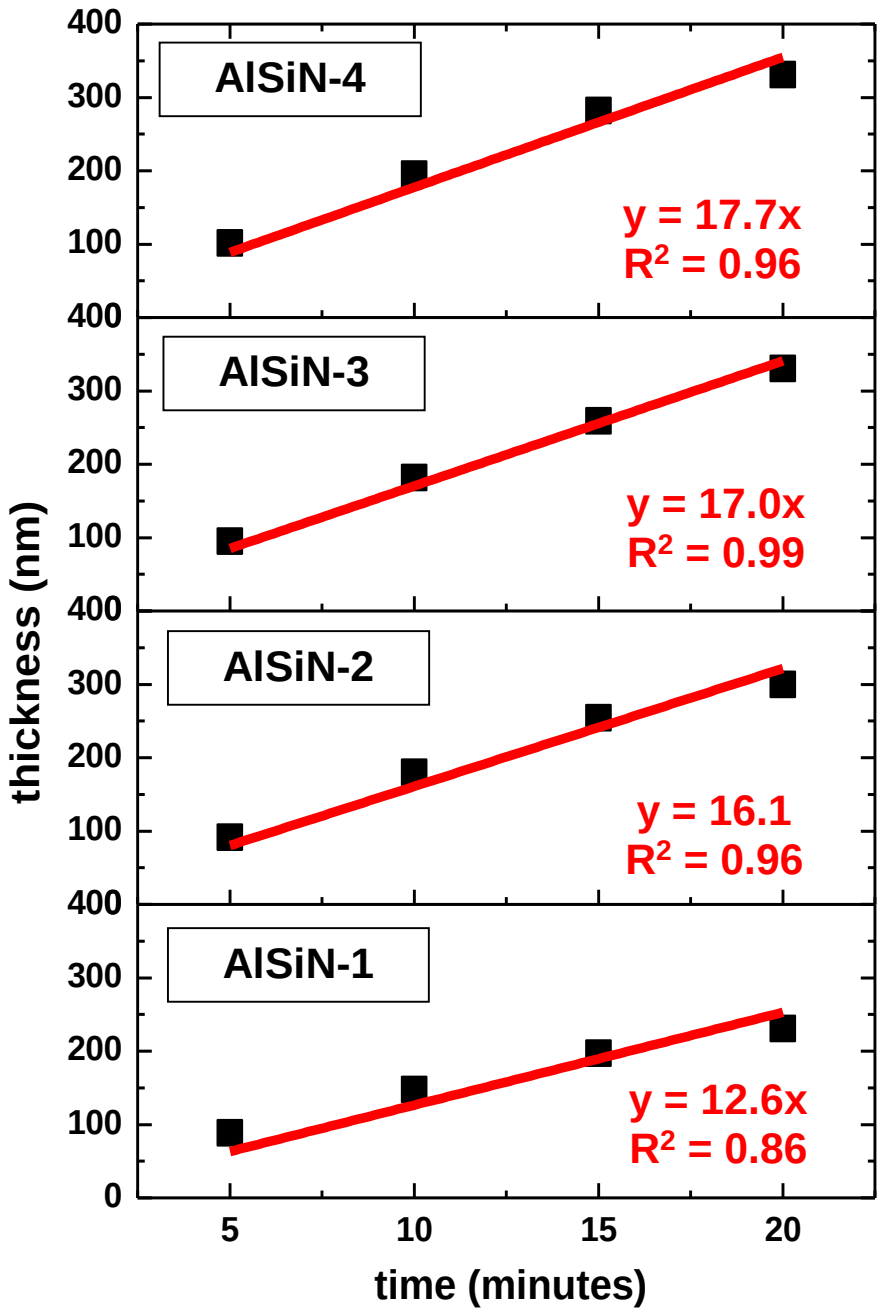

Figure 7. Thickness versus time of Al-Si-N films deposited using different AlSi composite targets.

Table 3. Thickness measurements of films deposited at RT

	Thickness (nm)			
Point #	**AlSiN-1**	**AlSiN-2**	**AlSiN-3**	**AlSiN-4**
1	746	801	775	775
2	740	798	787	788
3	729	803	785	792
average	**738**	**801**	**782**	**785**

Table 4. Thickness measurements of films deposited at 200^{o}C

	Sample			
Sample #	**AlSiN-1**	**AlSiN-2**	**AlSiN-3**	**AlSiN-4**
1	796	764	764	711
2	809	766	756	720
3	812	777	766	707
average	**806**	**769**	**762**	**713**

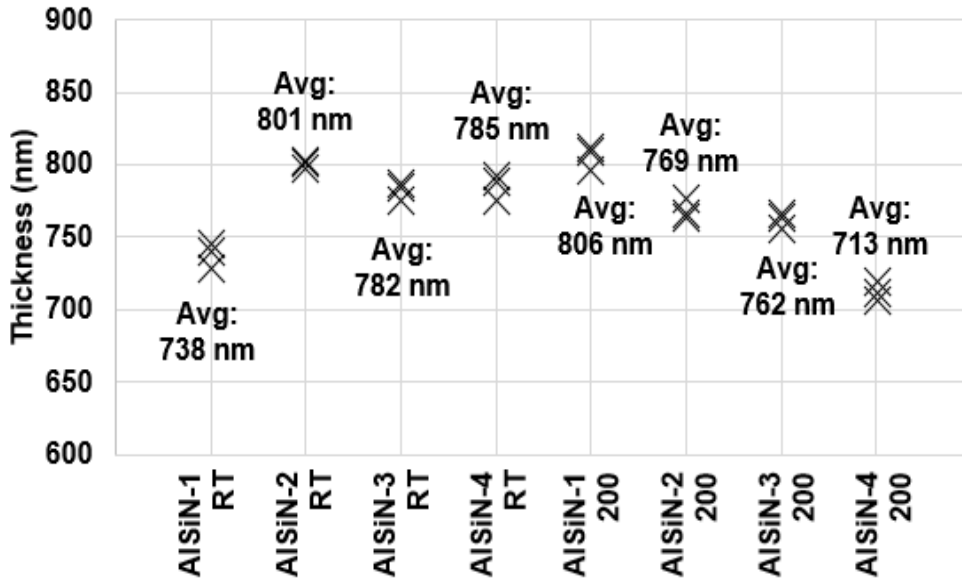

Figure 8. Plot of AlSiN film thicknesses deposited with different silicon content and deposition temeprature

The effect of the substrate temperature during deposition on the transparency of the Al-Si-N film was compared. Films of different silicon content were deposited at both room temperature and 200^{o}C. The transmittance curve of the deposited films can be seen in Figures 9 to 12 for AlSiN-1, AlSiN-2, AlSiN-3, and AlSiN-4 respectively. For all the films, regardless of the silicon content, it can be seen that the films deposited at RT were of higher or similar transmittances compared to the films deposited at higher temperature. Transmittances are higher particularly in the visible range.

The differences in transmittance can be due to the presence of oxidation at higher temperatures. It has been noted by Verpek et al. that oxygen may diffuse at the interface of the nanocomposite films which may affect the transparency of the films, especially at elevated temperatures. [56]

The transmittance curves for films of all compositions deposited at RT can be seen in Fig. 13

It can be seen that the films have similar transmittance levels regardless of the silicon content.

The hardness values of the deposited films at RT were measured and compared. The hardness values of the films can be seen in Table 5.

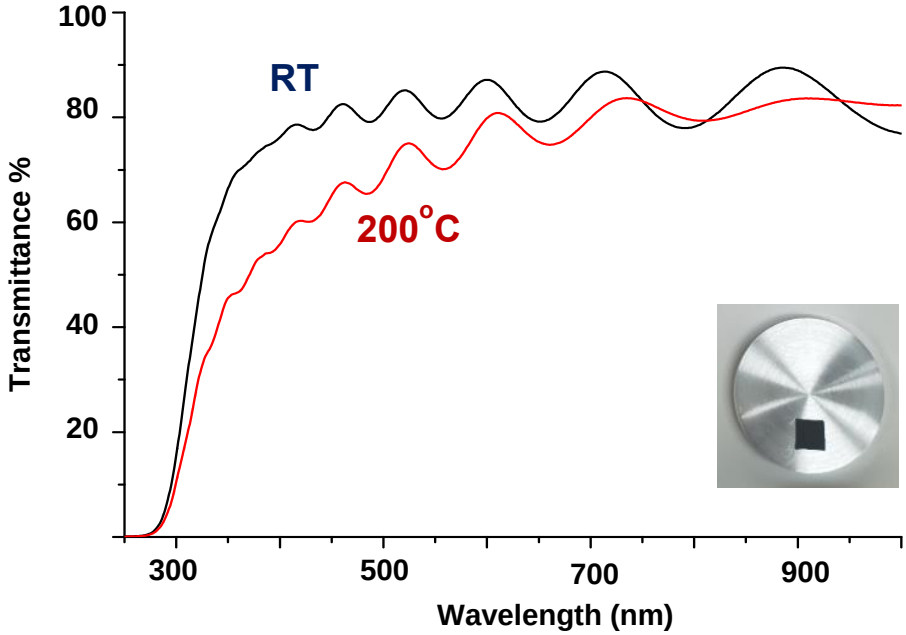

Figure 9. Optical transmittance curves of Al-Si-N films deposited using AlSi-1 target at different substrate temperatures

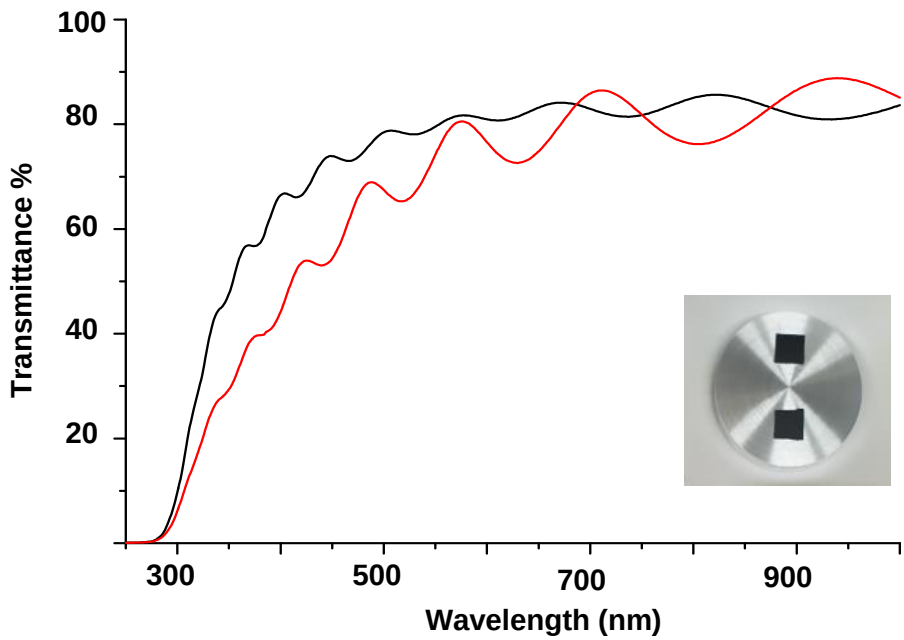

Figure 10. Optical transmittance curves of Al-Si-N films deposited using AlSi-2 target at different substrate temperatures

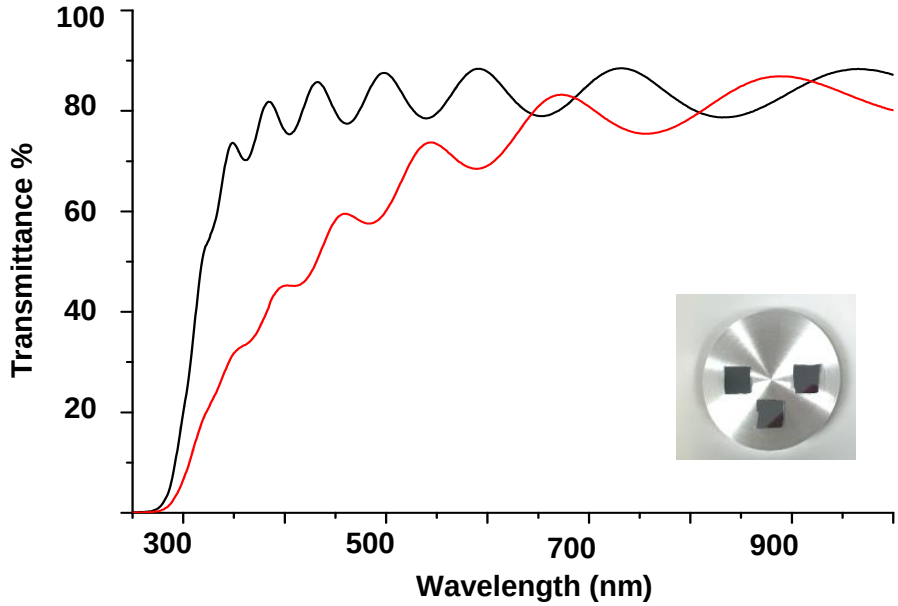

Figure 11. Optical transmittance curves of Al-Si-N films deposited using AlSi-3 target at different substrate temperatures

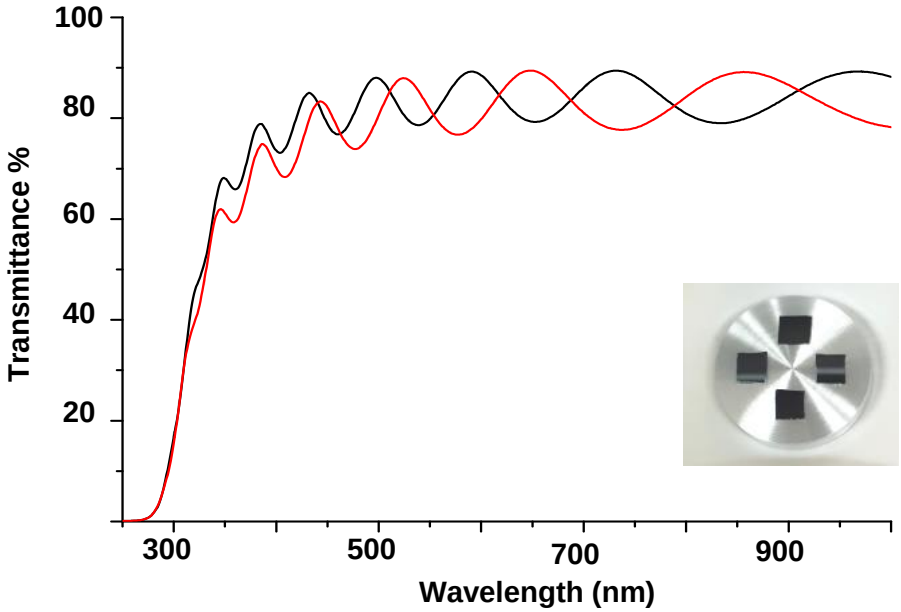

Figure 12. Optical transmittance curves of Al-Si-N films deposited using AlSi-1 target at different substrate temperatures

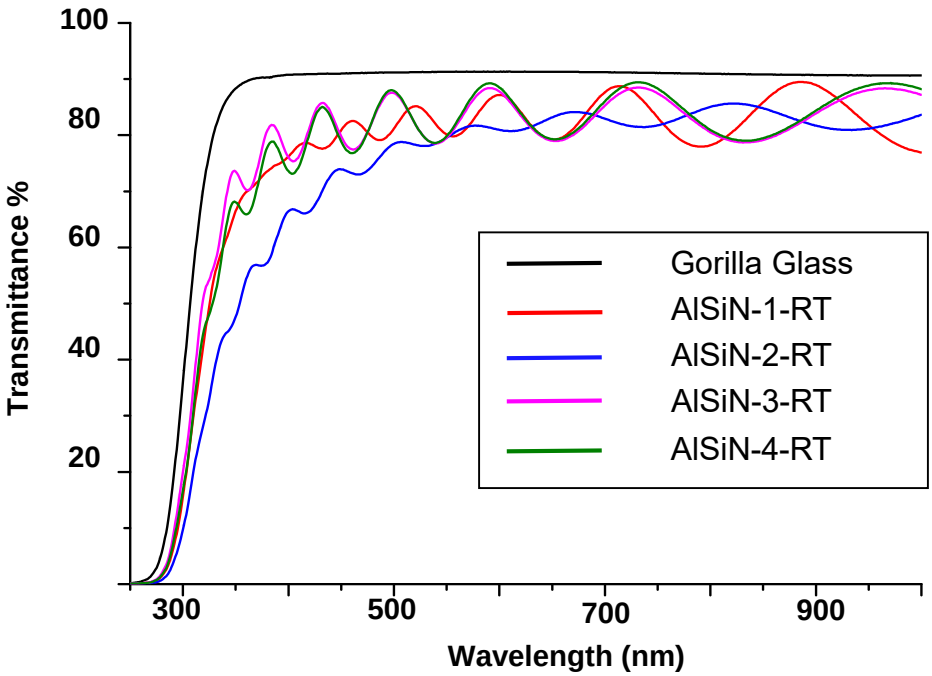

Figure 13. Transmittance curves for Al-Si-N films deposited at RT

Table 5. Hardness values of Al-Si-N films with different silicon composition

Specimen	Hardness (GPa)
AlSiN1-RT	20.7 ± 1.3
AlSiN2-RT	15.9 ± 0.7
AlSiN3-RT	15.2 ± 0.7
AlSiN4-RT	15.1 ± 0.3

As the silicon content increases, the hardness value decreases. There is a maximum value of 20.7 GPa attained for AlSiN-1. AlSiN-1 could possibly have the highest hardness value due to the film having a nanocomposite structure while the other films may have be of AlN and Si_3N_4 solid solution since they are of higher silicon content. It was found in later experiments that the silicon content of the films deposited with AlSiN-1 have silicon contents of ~15 at%, which is within the range of films with nanocomposite structures. The higher silicon content of AlSiN 2-4 films could have surpassed the content limit for films to have the nanocomposite structure and thus have lower hardness.

4.2. Effect of Film Thickness

4.2.1. Thickness Measurements

Given the selected parameters used during the previous experiments, Al-Si-N films with three different thicknesses were deposited using AlSi-1 target at room temperature. At least three films per thickness were deposited. The thickness of all films can be seen in Table 6.

Films of ~0.6, ~0.8, and ~1 μm were successfully deposited.

Table 6. Thickness of deposited samples

Sample thicknesses (nm)			
Sample #	**Sample thickness set**		
	1	**2**	**3**
1	629	822	1054
2	645	821	1110
3	617	935	990
4	650	949	
average	**630**	**881**	**1051**

4.2.2. EDS Analysis

The relative compositions of all the films were measured through EDS. The measured films were deposited on stainless steel. The relative compositions of films with ~0.6, ~0.8, and ~1 μm thicknesses may be seen in Tables 7, 8, and 9 respectively

Table 7. Relative Compositions of Al-Si-N Films with ~0.6 μm thickness

Sample	Al (at %)	Si Al (at %)	N Al (at %)
630-1	70.39	13.79	15.81
630-2	72.42	15.02	12.57
630-3	71.08	13.97	14.94
630-4	71.75	13.14	15.10
average	**71.41**	**13.98**	**14.60**

Table 8. Relative Compositions of Al-Si-N Films with ~0.8 μm thickness

Sample	Al (at %)	Si Al (at %)	N Al (at %)
860-1	68.12	16.90	14.98
860-2	71.86	16.57	11.57
860-3	70.62	14.62	14.76
860-4	71.70	14.85	13.45
average	**70.57**	**15.73**	**13.69**

Table 9. Relative Compositions of Al-Si-N Films with ~1 μm thickness

Sample	Al (at %)	Si Al (at %)	N Al (at %)
1050-1	67.43	15.35	17.24
1050-2	72.03	15.62	12.35
1050-3	69.30	14.24	16.46
average	**69.59**	**15.07**	**15.35**

According to the results, all films, regardless of thickness, are of similar relative compositions. All films have an average of 70.63 at% Al, 14.92 at% Si, and 14.54 at% N.

Since the films have a relative composition of 15 at %, the films should be of nanocomposite structure.

4.2.3. SEM Analysis

The surface morphologies of the films were observed through FESEM. The morphologies of films with ~0.6, ~0.8, and ~1 μm thicknesses may be seen in fig.14a to fig. 14c respectively.

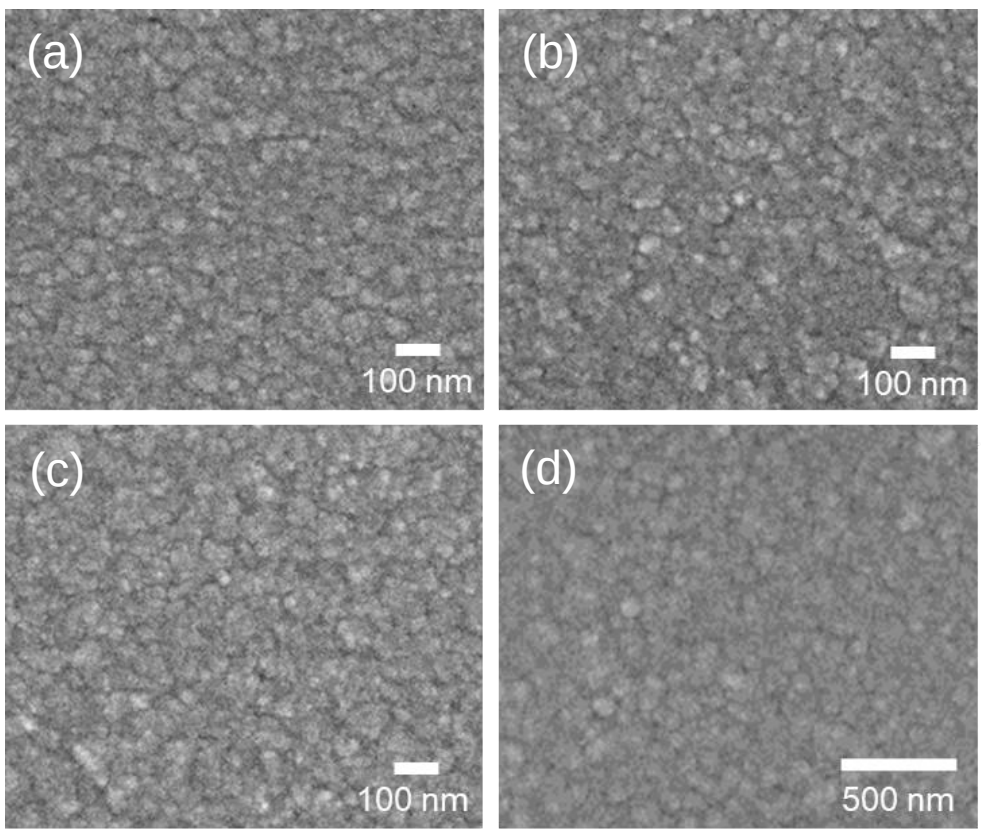

Figure 14. FESEM images of the surface morphology of Al-Si-N films. (a) film of ~ 0.6 μm thickness (b) film of ~ 0.8 μm thickness (c) film of ~ 0.8 μm thickness (d) Al-Si-N nanocomposite film from Liu et al.

The surface morphologies of the films, regardless of the thickness, are similar to each other. The films are observed to have a grainy morphology with grains sizes less than 100 nm.

The surface morphology of Al-Si-N film by Liu et al. may be seen in fig.14d. This film is with silicon content of 19 at % and was deposited through RF magnetron sputtering. Liu et al. reported that the deposited film was of nanocomposite structure.

When compared with the deposited films of this study, it can be seen that the surface morphologies of the films are similar to each other. It can be said that the films deposited in this study can be of nanocomposite structure as well.

4.2.4. XRD Analysis

Al-Si-N films deposited on Gorilla Glass were analysed through X-ray diffraction (XRD). Fig. 15 shows the X-ray diffraction patterns of the Al-Si-N films of varying thicknesses. All films, regardless of their thicknesses, have the same patterns and show the same peaks. Fig. 16 shows the XRD patterns of one representative sample per thickness. The XRD patterns match well with the pattern of AlN showing AlN crystalline peaks at (100),

(101) and (110). This possibly shows the presence of AlN nanocrystallites in the system.

This result matches with the results presented by Liu et.al. and is different from the results showed by Pelisson et al. and Musil et. al. Liu et al. presented XRD patterns of different Si content with preferred texture of (100), similar to the results of this research as compared to the results of Pelisson et al. which showed a result of a preferred peak of (002). Results by Musil et al. and Sergeev et al. also show similar results to Pelisson et al.

The differences in the preferred crystallographic orientation can be attributed to the type of deposition equipment and method used. Musil and Pelisson's team used either an unbalanced or a closed magnetic field dual magnetron sputtering system which can deliver energetic ions on the growing film. Unlike these systems, balanced magnetron sputtering systems give of ions of lower energies which induces much less energetic depositions of films. Xu et al. has reported that sputtering power can change the preferential orientation of AlN films. [19, 24, 57]

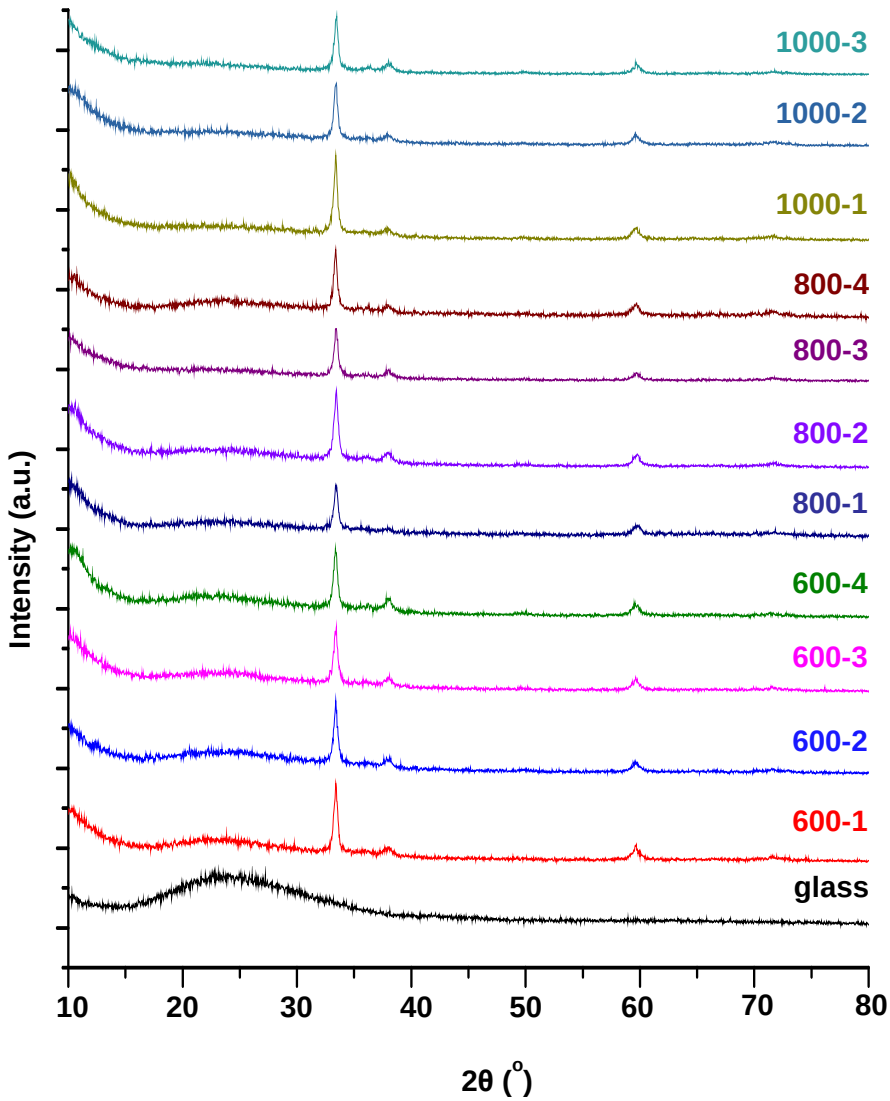

Figure 15. XRD patters of all the samples

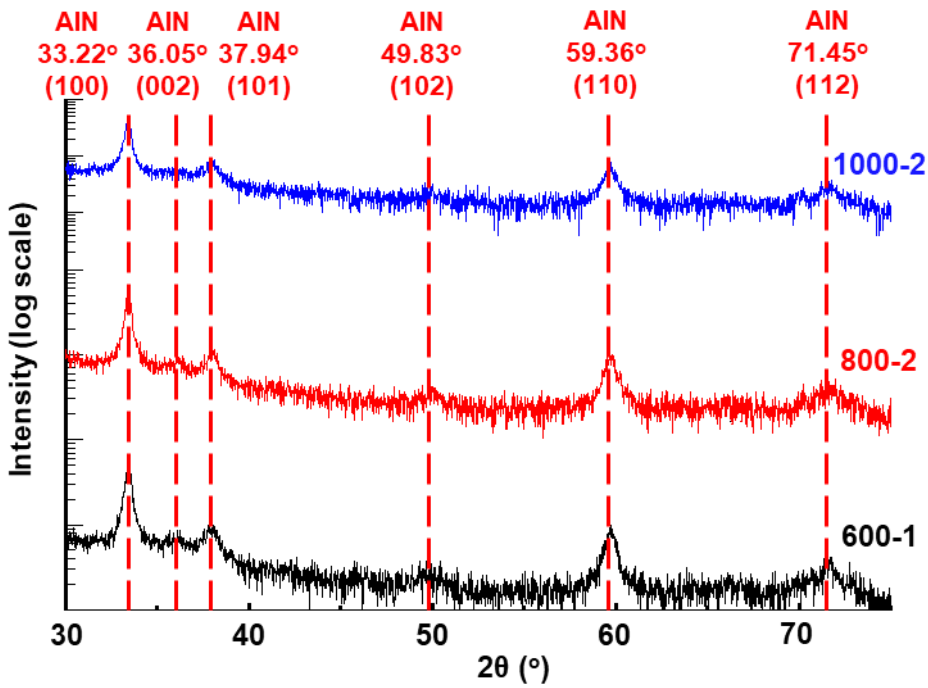

Figure 16. XRD patters of selected samples

4.2.5. UV Vis Spectroscopy Analysis

The transparency of the films deposited on glass were compared. The images of the films on glass may be seen in fig. 17. All the films deposited are transparent to the naked eye.

The transmittances of each film were measured using a UV-Vis spectrometer. The transmittance values from 250 to 1100 nm of films of ~0.6, ~0.8, and ~1 μm are seen in figs. 18 to 20 respectively. Films with similar thicknesses are found to have similar transmittance values. There are slight variations of the transmittance curves of films with similar thicknesses. This is due to their small differences in thickness. It can also be seen that all films possess interference fringes all throughout the measured spectrum. This is due to the interference of the reflected light off the air-film and film-substrate interface.

The well-defined oscillations seen in the interference fringes indicates that the deposited films have a smooth and flat surface. This also shows that the films have uniform thicknesses. [58] This smoothness and uniform thickness may only be limited to the measured area during spectrophotometry. The beam cross section of the spectrophotometer used, which is the area that was measured, is 0.6 mm x 9 mm.

When compared, films with different thicknesses show slight differences in both amplitude and the frequency of the interference fringes as seen in fig. 21 and fig. 22 respectively. The interference pattern produced

by transparent films are dependent on the interaction of the reflected light from the air-film and film-substrate interfaces. The amount of reflected and transmitted light is dependent on the wavelength of the light and at the same time the properties of the film, particularly its thickness. [37, 38]

Even small changes in thickness can alter the interference pattern. Films with higher thickness produce interference patterns with more closely spaced fringes, especially at higher wavelengths. Films with thicker thicknesses also have fringes with higher amplitudes. This trend is shown in the results.

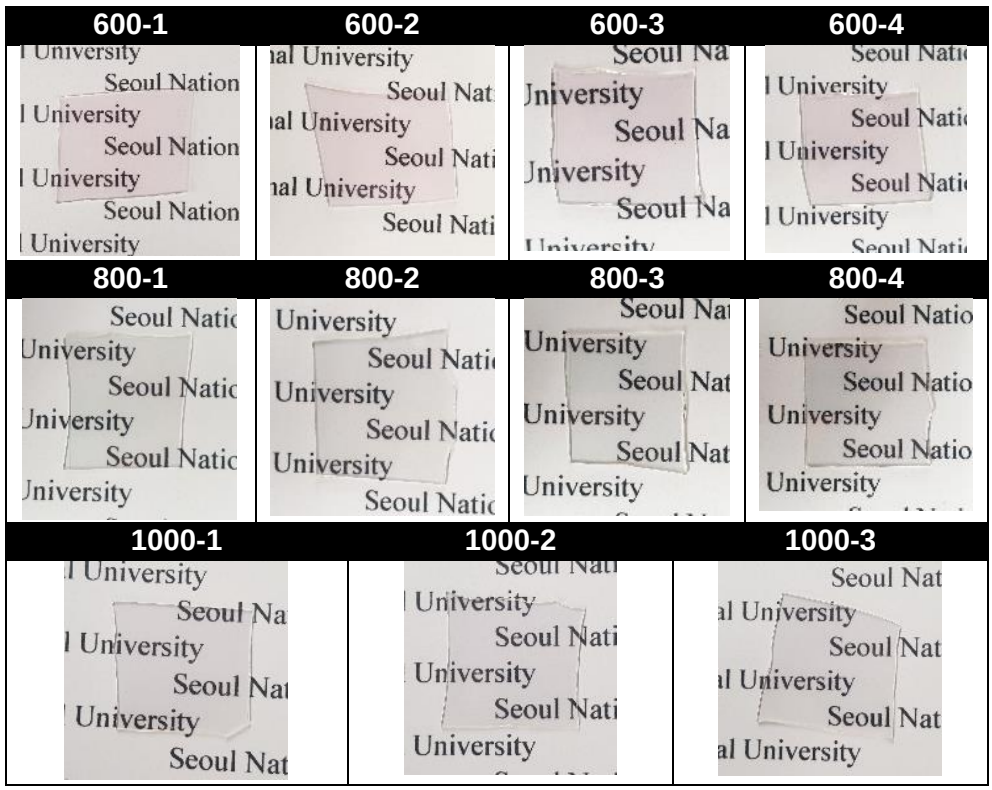

Figure 17. Images of the as-deposited films on Gorilla Glass

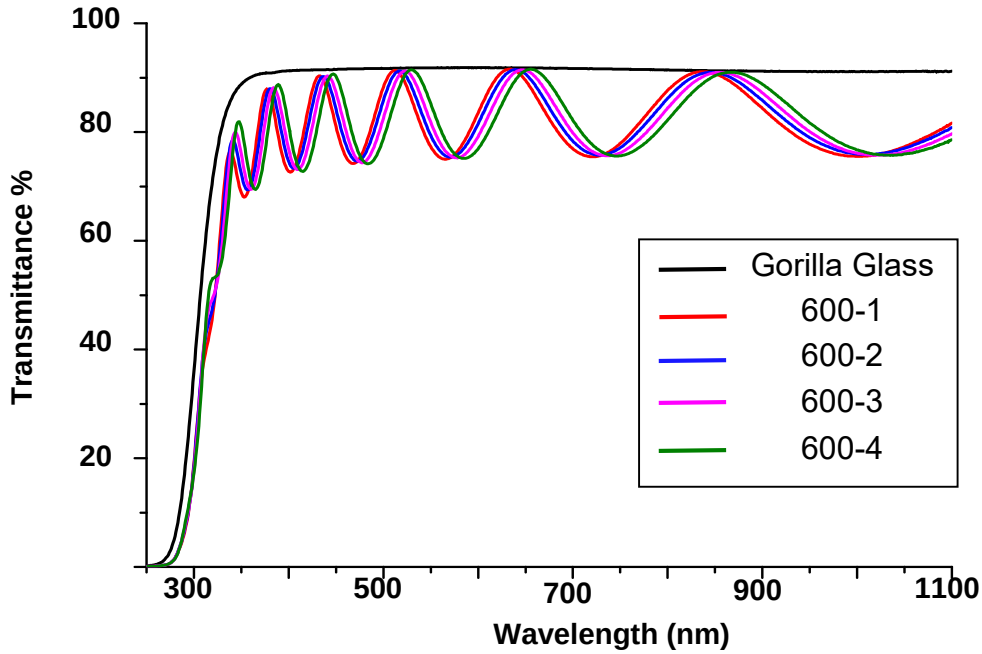

Figure 18. Optical transmittance curves of Al-Si-N films deposited using AlSi-1 target with ~0.6 μm thickness

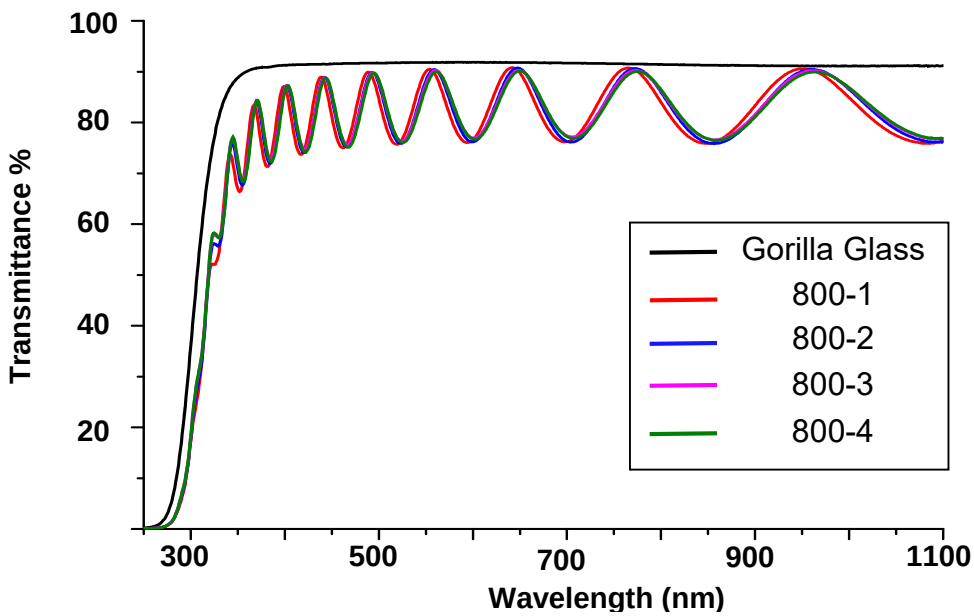

Figure 19. Optical transmittance curves of Al-Si-N films deposited using AlSi-1 target with ~0.8 μm thickness

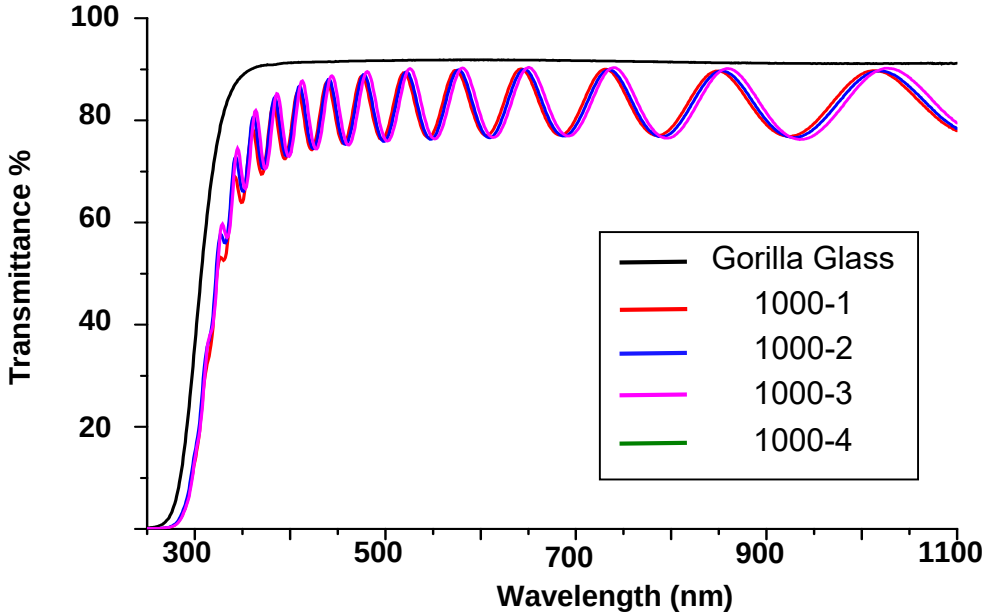

Figure 20. Optical transmittance curves of Al-Si-N films deposited using AlSi-1 target with ~1 μm thickness

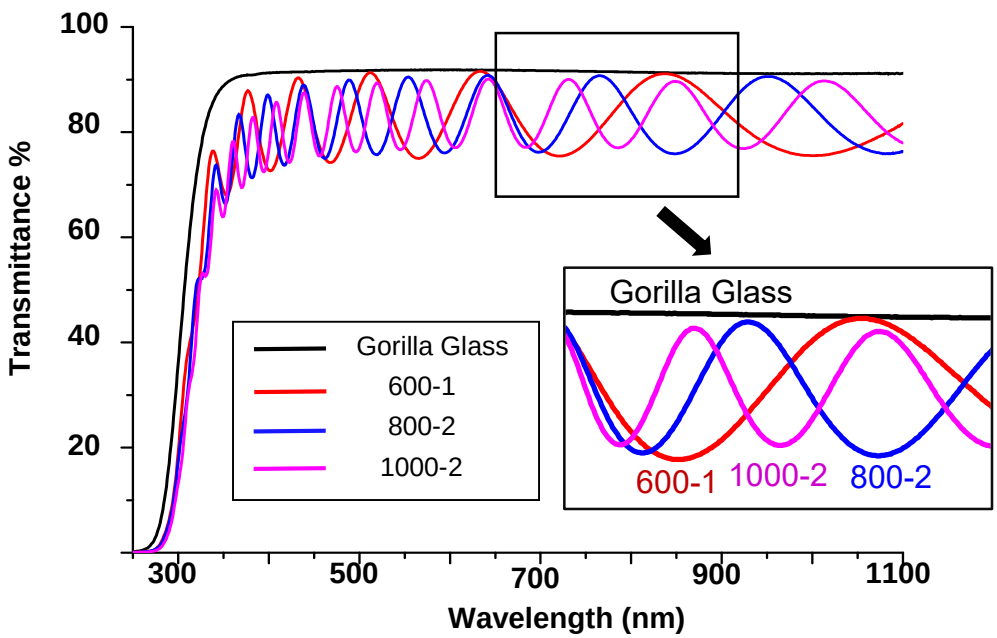

Figure 21. Optical transmittance curves of select Al-Si-N films.

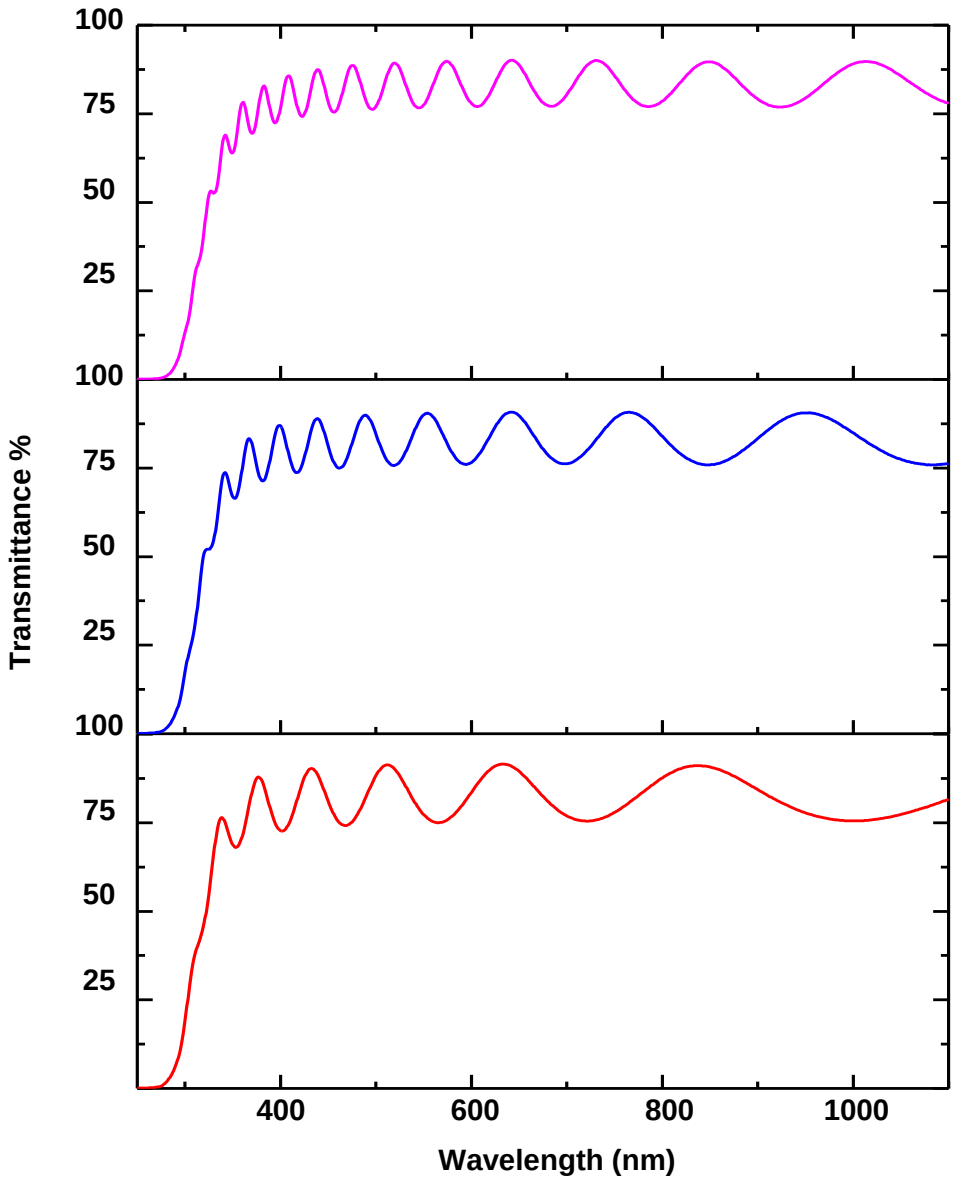

Figure 22. Optical transmittance curves of select Al-Si-N films.

4.2.6. Nanoindentation Analysis

The hardness values of the deposited Al-Si-N films were measured using nano-indentation. The hardness values of the films are seen in Table 10 and are graphed in fig. 23.

According to the results, most of the deposited films have a recorded hardness value higher than 16 GPa, the reported hardness for AlN. As shown in the previous results, the higher hardness values can be attributed to the nanocomposite structure of the film.

Films with ~0.6, ~0.8, and ~1 μm thicknesses have an average hardness values of 18.8 GPa, 17.0 GPa, and 20.7 GPa respectively. There is no evident overall trend of the hardness values versus thickness as there was a decrease and then increase of the hardness with increasing thickness.

It can also be seen that the hardness values of some films with similar thicknesses have comparatively large deviations. This can be due to fluctuations in the sputtering parameters during deposition as any small changes can lead to differences in the properties of the film. It may also be due to the unevenness in the composition of the deposited film. Since there was only one piece of silicon attached to one point of the target, the deposited film may contain uneven amounts of silicon over its area which can cause uneven properties, especially hardness.

The fluctuations in hardness values may also be due to different surface roughness over the area of the film. Although the well-defined interference fringes are an indication of smoothness and evenness of the films, it may only be limited to the analysis area during spectrophotometry. The films may have different roughness over areas larger than the cross section.

Even with the differences in hardness values, the hardness levels of the films are comparable. Films with ~0.6 μm thickness have similar hardness levels as compared to films with ~1 μm thickness. This shows that Al-Si-N films of thicknesses as low as ~0.6 μm can be applied to gorilla glass without compromising its hardness.

Table 10. Hardness Values of films with different thicknesses from nano-indentation

Sample #	Thickness (nm)		
	600 (GPa)	**800 (GPa)**	**1000 (GPa)**
1	21.2 ± 0.5	13.2 ± 0.3	21.9 ± 0.8
2	19.0 ± 1.1	21.4 ± 0.9	22.4 ± 1.0
3	14.2 ± 0.5	18.8 ± 0.7	17.7 ± 0.9
4	20.8 ± 0.8	14.5 ± 0.4	
average	**18.8 ± 3.2**	**17.00 ± 3.8**	**20.69 ± 2.6**

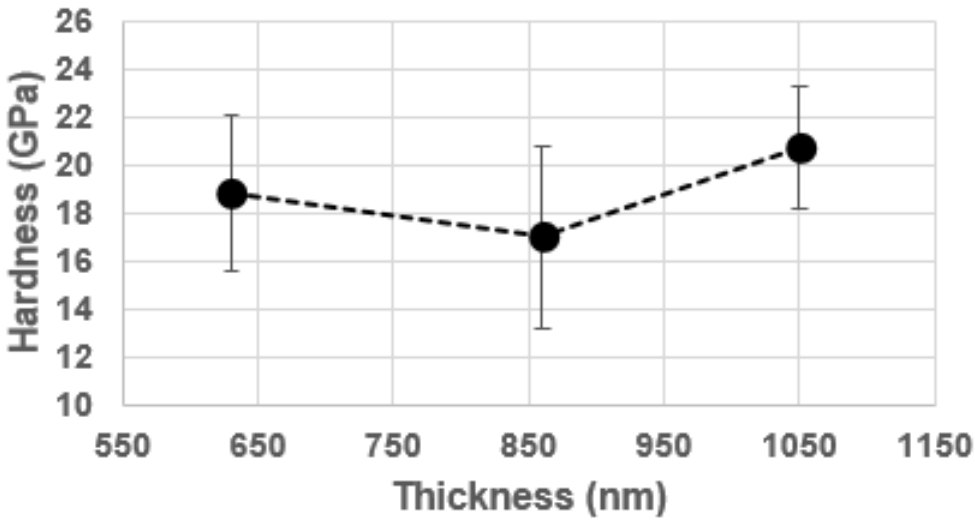

Figure 23. Trend of hardness values for different Al-Si-N thicknesses

5. Conclusions

The search for a possible material that can be applied to protect the displays of electronic devices such as cell phones while still possessing high transparency has gained due interest. In this study, the possibility of applying Al-Si-N films on gorilla glass and the effects of the silicon content and the thickness of the films on the optical property and hardness were determined.

Using RF reactive magnetron sputtering, Al-Si-N films of four different silicon contents were deposited using optimized sputtering parameters, and the hardness values and transparencies were compared. The films were deposited using different AlSi composite targets with different numbers of Si pieces attached to an Al target. It was shown that as the silicon content was increased, the hardness values of the films was decreased. This can come from the different microstructures with different silicon contents. The film deposited with the smallest amount of silicon was shown to have nanocomposite structure which can lead to the enhanced hardness of the film. The silicon content of the films did not have any significant influence on the transmittance levels of the films.

To determine the effect of thickness on the hardness values and transparencies of the films, Al-Si-N films of ~0.6, ~0.8, and ~1 μm were deposited. All the samples, regardless of the thickness, showed similar relative compositions with silicon contents of ~15 at %, which is typically the

silicon content of films with nanocomposite structures. XRD analyses show the presence of AlN crystallites, and the surface morphology was observed to be grainy and similar to those of previous reports of nanocomposite films.

The transmittance levels of the films with different thicknesses were similar. Oscillations of the transmittances (in different wavelengths) were seen in all samples which are due to the interference of light reflected from the air-film and film-substrate interfaces. This signifies the smoothness and evenness of the films. Though similar, there were slight changes to the fringe spacing and the amplitude of the oscillations. This is due to the thickness differences of the samples as these parameters are sensitive to any changes in thickness. Also, as the thickness was increased, there was a slight decrease in the transmittance of the films

Films with ~0.6, ~0.8, and ~1 μm thicknesses have an average hardness values of 18.8 GPa, 17.0 GPa, and 20.7 GPa, respectively. It was presented that films with ~0.6 nm thickness have the same hardness level as films with ~1 μm thickness. This shows that Al-Si-N films as thin as ~0.6 μm can be applied to Gorilla Glass and still maintain high hardness and transmittance values. Although the hardness levels of the films on average are similar, there were difference in hardness values for films of similar thicknesses. The difference can be due to uneven silicon contents over area of the film which can cause different hardness values at different points. It may also be due to different surface roughness at different points of the film.

While this study shows the feasibility of the application of Al-Si-N films on Gorilla Glass as a hard coating, there are still many improvements needed before the practical application of the films. It is recommended that in future studies, ways to increase the deposition rate should be studied as well as the ways to improve the hardness values of the films such as further optimization of composition. The regularity of the silicon content and surface roughness of the films should also be investigated. The transmittance levels of the films can also be further improved through methods such as choosing specific thicknesses that can reduce reflected light from the surfaces of the films.

6. References

1. MarketWatch. *Americans spent over $3 billion last year fixing their smartphone screens*. 2018 [cited 2019 June]; Available from: https://www.marketwatch.com/story/americans-spent-over-3-billion-last-year-fixing-their-smartphone-screens-2018-11-20.
2. Rayner, T. *You may not believe how many phone screens are cracked per hour*. 2018 [cited 2019 June]; Available from: https://www.androidauthority.com/cracked-phone-screen-927180/.
3. Callaham, J. *The race to 100%: How screen-to-body ratios changed over the years*. 2018 [cited 2019 June]; Available from: https://www.androidauthority.com/smartphone-screen-to-body-ratio-878835/.
4. Hoornaert, T., Z.K. Hua, and J.H. Zhang. *Hard Wear-Resistant Coatings: A Review*. 2010. Berlin, Heidelberg: Springer Berlin Heidelberg.
5. Çalışkan, H., P. Panjan, and C. Kurbanoglu, *Hard Coatings on Cutting Tools and Surface Finish*. 2017. p. 230-242.
6. Pelisson-Schecker, A., H.J. Hug, and J. Patscheider, *Morphology, microstructure evolution and optical properties of Al-Si-N nanocomposite coatings.* Surface & Coatings Technology, 2014. **257**: p. 114-120.

7. Crystalusion. *Liquid Glass Protector*. 2018 [cited June 2019]; Available from: https://crystalusion.com/liquid-glass-protector/.
8. Choi, H.-S., et al., *Hard-coating film for display device, and display device comprising same*, D.C.S.E.C. Ltd, Editor. 2016.
9. M. George, P.M., J. Morris, H. Chandra, J. Madocks, *Deposition of Silicon Oxide, Silicon Nitride and Silicon Carbide Thin Films by New Plasma Enhanced Chemical apor Deposition Source Technology* in *AIMCAL*. 2007. p. 1-12.
10. Nanning Arfsten, J.G., Brandon Steel, Kerrin Arfsten *Anti-reflection UV-blocking multilayer coatings having a thin film layer having cerium oxide, silicon dioxide and transition metal oxides*, D.T. LLC, Editor. 2004.
11. Panitchakan, H. and P. Limsuwan, *Characterization of Aluminum Oxide Films Deposited on Al2O3-TiC by RF Diode Sputtering.* Procedia Engineering, 2012. **32**: p. 902-908.
12. Rüger, M., *Plastics with a Touch of Glass*, Schott, Editor. 2002: Munich. p. 18-20.
13. Tingjun XU, X.Z., Wookyung BAE, Sunggu Kang, John Z. Zhong *Electronic Devices with Sapphire-Coated Substrates*, A. Inc., Editor. 2016: United States.
14. van der Rest, A., et al., *Mechanical behavior of ultrathin sputter deposited porous amorphous Al2O3 films.* Acta Materialia, 2017. **125**: p. 27-37.

15. 우창수, 하., 문형랑, 이우진, 장승우, 전환승, 한동일, *Hard coating liquid composition and polycarbonate glazing using same*, 삼. 주식회사, Editor. 2014.

16. Bozhko, I., et al., *Microstructure and properties of nanocomposite Al-Si-N system coatings produced by magnetron sputtering.* AIP Conference Proceedings, 2016. **1772**(1): p. 030014.

17. Bozhko, I.A., et al., *Investigation of the structural-phase state and the impact-protective properties of optically transparent Si-Al-N coatings.* AIP Conference Proceedings, 2015. **1683**(1): p. 020028.

18. Bozhko, I.A., et al., *Protection from high-velocity impact particles for quartz glass by coatings on the basis of Al-Si-N.* AIP Conference Proceedings, 2016. **1783**(1): p. 020018.

19. Liu, H., et al., *Characterization of (Al, Si)N films deposited by balanced magnetron sputtering.* Thin Solid Films, 2009. **517**(21): p. 5988-5993.

20. Mishra, S.K., S. Kumari, and Soni, *Development of hard and optically transparent Al-Si-N nanocomposite coatings.* Surface and Interface Analysis, 2017. **49**(4): p. 345-348.

21. Musil, J., et al., *Effect of energy on the formation of flexible hard Al-Si-N films prepared by magnetron sputtering.* Vacuum, 2016. **133**: p. 43-45.

22. Musil, J., et al., *Flexible hard Al-Si-N films for high temperature operation.* Surface & Coatings Technology, 2016. **307**: p. 1112-1118.

23. Musil, J., et al., *Properties of magnetron sputtered Al–Si–N thin films with a low and high Si content.* Surface and Coatings Technology, 2008. **202**(15): p. 3485-3493.

24. Pelisson, A., et al., *Microstructure and mechanical properties of Al-Si-N transparent hard coatings deposited by magnetron sputtering.* Surface & Coatings Technology, 2007. **202**(4-7): p. 884-889.

25. Sergeev, V., et al., *Magnetron sputtering of Si-Al-N nanocomposite coatings on quartz for protection against impacts of high speed microparticles.* Vacuum, 2017. **143**: p. 454-457.

26. Zenkin, S., et al., *Structure, Mechanical and Optical Properties of Silicon-Rich Al–Si–N Films Prepared by High Power Impulse Magnetron Sputtering.* Coatings, 2019. **9**(1): p. 53.

27. Bunshah, R.F. and C.V. Deshpandey, *Hard coatings.* Vacuum, 1989. **39**(10): p. 955-965.

28. Wei, R., et al., *Deposition of thick nitrides and carbonitrides for sand erosion protection.* Surface and Coatings Technology, 2006. **201**(7): p. 4453-4459.

29. Corning, *Gorilla Glass Product Information*, Corning, Editor. 2018.

30. Vepřek, S., *The search for novel, superhard materials.* Journal of Vacuum Science & Technology A, 1999. **17**(5): p. 2401-2420.

31. Project, M. *Si3N4 (hexagonal)*. 2019 [cited 2019 June]; Available from: https://materialsproject.org/materials/mp-988/.

32. Klimm, D., *Electronic materials with a wide band gap: recent developments.* IUCrJ, 2014. **1**(5): p. 281-290.

33. Lewin, E., et al., *Comparison of Al–Si–N nanocomposite coatings deposited by HIPIMS and DC magnetron sputtering.* Surface and Coatings Technology, 2013. **232**: p. 680-689.

34. Kasu, M., Y. Taniyasu, and N. Kobayashi, *Formation of Solid Solution of Al1-xSixN (0<x≤ 12%) Ternary Alloy.* Japanese Journal of Applied Physics, 2001. **40**(Part 2, No. 10A): p. L1048-L1050.

35. López, J.M., et al., *Low grain size TiN thin films obtained by low energy ion beam assisted deposition.* Applied Surface Science, 2001. **173**(3): p. 290-295.

36. Kariper, İ.A., *Hardness of Thin Films and the Influential Factors*, in *Diamond and Carbon Composites and Nanocomposites*, M. Aliofkhazraei, Editor. 2016, IntechOpen.

37. Gu, B. and H.-T. Wang, *inear and Nonlinear Optical Properties of Ferroelectric Thin Films.* Ferroelectrics - Physical Effects, 2011.

38. III, A.E.-R.F.D.B., *Thin Film Technology Handbook*, ed. C.A. Harper. 1998, United States of America: McGraw-Hill.

39. Ohring, M., *The Materials Science of Thin Films*. 1992, United States of America: Academic Press.

40. Gabriel, C.J. and A. Nedoluha, *Transmittance and Reflectance of Systems of Thin and Thick Layers.* Optica Acta: International Journal of Optics, 1971. **18**(6): p. 415-423.

41. Kataria, S., et al., *Nanocrystalline TiN coatings with improved toughness deposited by pulsing the nitrogen flow rate.* Surface and Coatings Technology, 2012. **206**(19): p. 4279-4286.

42. Kelly, P.J. and R.D. Arnell, *Magnetron sputtering: a review of recent developments and applications.* Vacuum, 2000. **56**(3): p. 159-172.

43. Maurya, D.K., A. Sardarinejad, and K. Alameh, *Recent Developments in R.F. Magnetron Sputtered Thin Films for pH Sensing Applications—An Overview.* Coatings, 2014. **4**(4): p. 756-771.

44. Mahan, J.E., *Physical Vapor Deposition of Thin Films*. 2000, Canada: John Wiley & Sons, Inc.

45. Zexian, C. *Radio Frequency Magnetron Sputtering*. 2000 [cited 2019 June]; Available from: http://surface.iphy.ac.cn/sf03/sputtering.htm.

46. Hughes, M. *What is RF Sputtering?* 2016 [cited 2019 June]; Available from: http://www.semicore.com/news/92-what-is-rf-sputtering.

47. Tadjine, R., M.M. Alim, and M. Kechouane, *The erosion groove effects on RF planar magnetron sputtering.* Surface and Coatings Technology, 2017. **309**: p. 573-578.

48. Peng, S., et al., *Influences of the RF power ratio on the optical and electrical properties of GZO thin films by DC coupled RF magnetron sputtering at room temperature.* Physica B: Condensed Matter, 2016. **503**: p. 111-116.

49. Ait-Djafer, A.Z., et al., *Deposition and characterization of titanium aluminum nitride coatings prepared by RF magnetron sputtering.* Applied Surface Science, 2015. **350**: p. 6-9.

50. Feng, L.-p., et al., *Influence of RF power on structure and electrical properties of sputtered SrHfON thin films.* Materials Letters, 2012. **78**: p. 66-68.

51. Ahmadipour, M., et al., *Structural, surface morphology and optical properties of sputter-coated CaCu3Ti4O12 thin film: Influence of RF magnetron sputtering power.* Materials Science in Semiconductor Processing, 2017. **66**: p. 157-161.

52. Chaoumead, A., Y.-m. Sung, and D.-J. Kwak, *The Effects of RF Sputtering Power and Gas Pressure on Structural and Electrical Properties of ITiO Thin Film.* Advances in Condensed Matter Physics, 2012. **2012**: p. 7.

53. Arif, M. and C. Eisenmenger-Sittner, *In situ assessment of target poisoning evolution in magnetron sputtering.* Surface and Coatings Technology, 2017. **324**: p. 345-352.

54. Fischer, M., et al., *A setup for arc-free reactive DC sputter deposition of Al-O-N.* Surface and Coatings Technology, 2019. **362**: p. 220-224.

55. Project, M. *AlN (hexagonal)*. 2019 [cited 2019 June]; Available from: https://materialsproject.org/materials/mp-661/.

56. Veprek, S., et al., *Degradation of superhard nanocomposites by built-in impurities.* Journal of Vacuum Science & Technology B: Microelectronics and Nanometer Structures Processing, Measurement, and Phenomena, 2004. **22**(2): p. L5-L9.

57. Xu, X.-H., et al., *Morphological properties of AlN piezoelectric thin films deposited by DC reactive magnetron sputtering.* Thin Solid Films, 2001. **388**(1): p. 62-67.

58. Kaur, G., A. Mitra, and K.L. Yadav, *Pulsed laser deposited Al-doped ZnO thin films for optical applications.* Progress in Natural Science: Materials International, 2015. **25**(1): p. 12-21.

국문 초록

하드 코팅은 표면 처리 기법 중 하나로, 높은 경도와 우수한 내마모성을 가지고 있어 외부 충격이나 강한 스크래치로부터 재료를 보호하는 역할을 한다. 따라서 공구, 엔진 등 다양한 분야에서 널리 활용되고 있다. 최근에는 smart-phone, smart-watch, 네비게이션 등 IT 기기 분야에서도 활용도가 커지고 있다. 터치패널이 내장된 디스플레이가 적용된 이들 기기는 사용자의 잦은 접촉으로 인해 외부 스크래치 및 환경에 민감하게 반응하고 손상이 발생되는 경우가 많다. 따라서 디스플레이의 cover-glass 표면에 하드 코팅 처리를 하여 외부 충격으로부터 보호하는 것이 중요하다.

현재 많이 사용되고 있는 하드 코팅 재료의 대부분은 가시광선 영역에서 낮은 투과율을 갖는다. 또한 표면 경도가 12GPa 정도의 수준으로 외부 충격으로부터 완전하게 디스플레이를 보호하기 어렵다.

따라서 본 연구에서는 최소한의 두께로 높은 수준의 경도를 가지면서, 가시광선 영역에서 높은 투과율을 가질 수 있는 Al-Si-N nanocomposite 박막을 제조하고자 하였다. 최신 모바일 기기의 cover-glass 로 사용되는 Gorilla 5 Glass 기판 위에 RF 마그네트론 스퍼터링 공정을 사용하여 박막을 제조하였고, Al-Si-N 의 조성과 두께에 따라 박막의 투과율 변화를 조사하였다.

Si 함량을 변화 시켜가면서 박막의 미세구조를 관찰하였다. Si 함량이 증가할수록 박막의 미세구조가 달라지고, 박막의 경도가 떨어지는 것을 확인하였다. 두께가 미치는 영향을 측정하기 위해 일정한 조성으로 0.6 다 Si-

0.8μ m, 1μ m 두께의 박막을 제조했다. 분석 결과, 두께와 관련 없이 제조된 박막은 모두 22GPa 정도의 높은 경도를 보였다. 또한 제조된 박막은 조성 및 박막의 두께와 관련없이 모두 90% 정도의 비슷한 가시광선 투과율을 가지는 것으로 나타났다.

본 연구를 통해 제조된 Al-Si-N 박막은 0.6μ m 의 얇은 두께로도 높은 경도를 구현하였으며, Glass 기판과 유사한 90% 정도의 높은 가시광선 투과율을 보였다. 따라서 IT 기기에 적용할 수 있는 최적의 하드 코팅이 될 수 있다고 판단하였다.

키워드: Al-Si-N, 하드 코팅, Gorilla Glass, 경도, 광학적특성, 투명도, 스퍼터링

학생번호: 2017-21243